

# ECONOMIC GEOLOGY

AND THE

BULLETIN OF THE SOCIETY OF ECONOMIC GEOLOGISTS

VOL. 87

NOVEMBER, 1992

No. 7

## Geology and Geochemistry of Wall-Rock Alteration at the Carlin Gold Deposit, Nevada

C. A. KUEHN AND A. W. ROSE

*Department of Geosciences, Pennsylvania State University, University Park, Pennsylvania 16802*

### Abstract

The Carlin disseminated gold deposit occurs in an autochthonous sequence of Paleozoic sedimentary rocks exposed in a structural window in the Roberts Mountains thrust in north-central Nevada. The upper 175 m of the Silurian Roberts Mountains Formation hosts the majority of ore at Carlin and is characterized by laminated, fine-grained, calcareous and/or dolomitic argillaceous siltstone with local coarser grained siltstones and <0.25- to >50-cm-thick lenticular interbeds of sand- and granule-sized calcareous bioclastic debris or fossil hash. Detailed studies of drill core and exposures in the East pit of the Carlin mine show that alteration and mineralization are zoned away from crosscutting fault conduits and these more permeable bioclastic beds, indicating that these two features were major inflow zones for hydrothermal fluid.

In unoxidized rocks, unaltered calcareous siltstone (1) containing quartz, dolomite, calcite, illite, K feldspar, and pyrite is progressively converted to assemblages of (2) quartz + dolomite + calcite + illite + pyrite, (3) quartz + dolomite + illite-K mica + pyrite, (4) quartz + illite-K mica + pyrite, and (5) quartz + kaolinite-dickite + pyrite adjacent to inflow zones where jasperoids are developed. Gold most consistently enriches the zone of calcite and dolomite removal (3 and 4 above), though it occurs in all zones, locally in high concentrations. This zoned alteration was accomplished by a CO<sub>2</sub>-rich acidic fluid. This acidic alteration enhanced the passage of fluids by extensive carbonate removal to form zones of higher permeability.

Oxidation is wholly a supergene effect related to deep weathering, because the oxidation is superimposed on both mineralized and altered rocks with only minor effect on the major element chemistry; it has produced low-temperature goethitic Fe oxides rather than higher temperature hematite and is not spatially related to Au distribution at the mine or on a district scale.

Because of extensive carbonate removal leading to local volume reduction through collapse and/or compaction, geochemical effects are examined using ratios to relatively immobile elements such as Al and Ti. Extensive depletion of Ca, Mg, and CO<sub>2</sub> and introduction of Si, Au, and S have occurred. Potassium is depleted in the conversion of illite to dickite-kaolinite in proximal silicified inflow zones, and Fe enriches some pyritized rock. Carbonate removal and silicification are two separate processes, both of which are spatially associated with mineralization. Mineralized decarbonated rocks and barren footwall rocks commonly are not silicified, and intensely silicified proximal alteration zones are generally low grade.

### Introduction

THE Carlin gold deposit, discovered in 1962, has produced more than 4 million ounces (125 t) of Au and is the type deposit of the most important group of Au mines developed in the United States since 1940. The deposit is located in north-central Nevada in the Lynn-Pinon mineral belt (Roberts, 1960), more recently referred to as the "Carlin trend." This N 35°-

40° W-trending feature represents the axial trace of the Tuscarora anticline (Madrid and Bagby, 1986) and contains at least 15 gold deposits of Carlin and related types along its 60-km length. These deposits have combined mined and unmined resources of greater than 2,000 t of Au (Knutsen et al., 1991), exceeding any other similar area in the United States. The Carlin deposit is located along the northern edge of the Lynn window in a northwest-trending zone of

hydrothermally altered rocks at least 0.8 km wide and nearly 7 km in length (Fig. 1).

Most previous models of mineralization and descriptions of hydrothermal alteration at Carlin are based largely on early exposures in the upper oxidized portions of the mine (Hausen and Kerr, 1968; Radtke et al., 1980; Radtke, 1985; Rye, 1985). This

paper presents results of a detailed study of unoxidized ores and host rocks from a series of drill cores from the Carlin East orebody and from less weathered exposures of the Carlin deposit than were previously available. The study of these unoxidized samples has allowed distinction of primary mineralization from supergene effects. In addition to

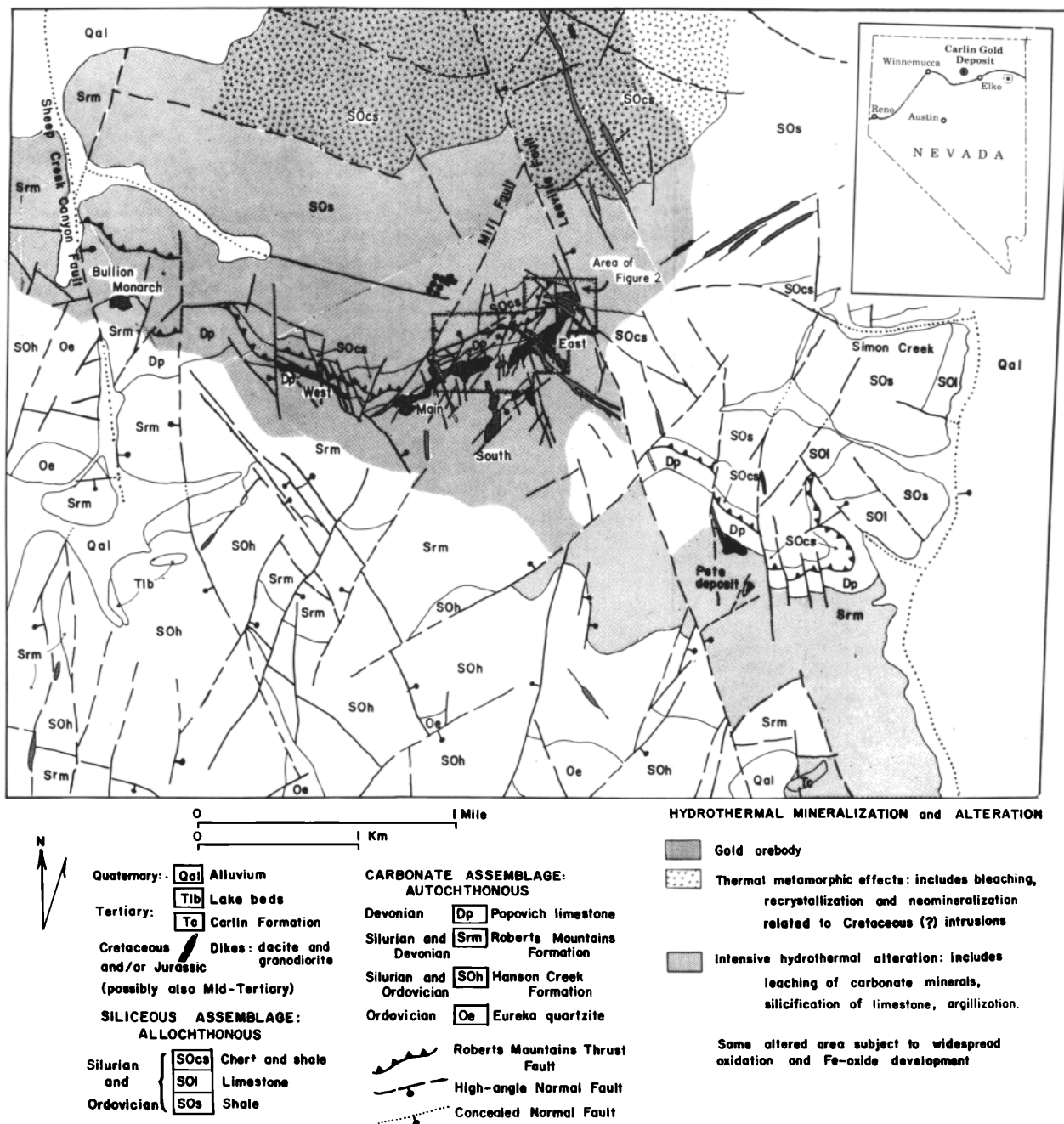


FIG. 1. Geologic map of the Carlin deposit and vicinity (after Evans, 1974a; Evans and Peterson, 1976; and Radtke, 1985).

mineralogical studies of alteration, major and trace element effects are also summarized by integrating new data and concepts with previous studies.

#### *Previous work*

The major alteration types previously described at Carlin are carbonate removal, silicification (jasperoid development), and argillization (Hausen, 1967; Hausen and Kerr, 1968; Evans, 1974a; Radtke et al., 1980; Radtke, 1985; Bakken and Einaudi, 1986; Armstrong et al., 1987). Most of these investigations lacked descriptions of the ores and altered rocks in terms of zoned mineral assemblages and also lacked detailed paragenetic studies. In addition, previous studies of chemical additions and depletions assume local conservation of either volume or mass which is concluded here and by Bakken (1990) to be invalid for many Carlin rocks (Akright et al., 1969; Radtke et al., 1972; Radtke et al., 1980; Radtke, 1985; Rye, 1985). Bakken and Einaudi (1986) demonstrated zoning from outer zones of carbonate removal to inner zones of silicification, but they were unable to evaluate changes in clays, sulfides, and carbonaceous matter because of pervasive superimposed oxidation in the Main pit where they mapped.

Hausen (1967, 1981, 1983, 1985), Hausen and Kerr (1968), and Hausen and Park (1986), as well as Radtke (1985), Radtke et al. (1980), and Rye (1985), suggest that the Carlin deposit formed in the epithermal environment in the roots of a hot spring-type hydrothermal system. Previous investigators at Carlin also concluded that relatively shallow boiling occurred at depths of less than 500 m. Condensation and oxidation of acidic volatile materials such as H<sub>2</sub>S in the upper levels of the deposit were interpreted to cause widespread hypogene acid leaching along with simultaneous oxidation of the host rocks (Radtke et al., 1980; Radtke, 1985; Rye, 1985). These earlier investigators also misinterpreted superimposed spatial associations, such as high organic carbon content and As values or acid leaching and oxidation, as implying a linkage in time of origin.

The distributions of Au and As, as well as features related to decalcification and silicification, are shown in cross section by Hausen et al. (1983). The spatial relationships of these same alteration characteristics for largely oxidized portions of the Main pit at Carlin have also been documented by Bakken and Einaudi (1986). All prior investigations at the Carlin deposit have concluded that portions of the upper mine exposures suffered from extensive oxidation, portions of which resulted from surficial alteration processes (Hausen and Kerr, 1968; Radtke et al., 1980; Radtke, 1985; Rye, 1985; Bakken and Einaudi, 1986). However, most previous investigators have not specified whether oxidation observed at any specified scale or in any specific sample is hypogene and concurrent

with mineralization, or supergene and significantly later than mineralization, or both.

#### *Methodology*

*Field studies:* Critical information was provided by 43 diamond drill cores completed in 1974–1975 from a drift beneath the East pit on the 6,260-ft level. These holes were drilled from the ends of 13 NS and 4 EW drill sections to evaluate the downdip extension of the East orebody (Fig. 2). During the present study, this core was logged in detail, and sample suites were chosen for geochemical analyses, carbonate staining and peels, petrography, scanning electron microscopy-energy dispersive spectrometry (SEM-EDS), X-ray diffraction (XRD), fluid inclusion measurements, and isotopic studies. The drill core array provided critical access to unoxidized footwall rocks up to 100 m below the ore and to geologic and alteration features spatially related to the downdip extension and closure of mineralization beneath the presently exposed levels of the open pit.

Field studies were conducted in the open pit in areas selected for detailed analytical work, including a continuous stratigraphic interval of carbon-rich ore containing numerous highly silicified beds (Fig. 2: 6,200-ft level, 23562 N, 20509 E), and an oxidized exposure of silicified, leached footwall rocks (Fig. 2: 6,200-ft level, 23503 N, 20958 E).

*Geochemical analyses:* Major element geochemistry was determined in the Mineral Constitution Laboratory at the Pennsylvania State University by direct current plasma-arc emission spectrochemical analysis (Medlin et al., 1969). Carbonate carbon and organic carbon analyses were obtained using a coulometer and a LECO carbon analyzer, respectively. Gold was determined by neutron activation (Bondar-Clegg Ltd.) and by standard fire assay methods (Carlin Gold Mining Co.; Analytical Services Co., Elko, Nevada; and Bondar-Clegg Ltd.). A complete listing of geochemical data for samples analyzed during the course of this study is available in Kuehn (1989).

### **The Carlin Gold Deposit**

#### *Geologic history*

An understanding of alteration associated with gold mineralization at Carlin requires understanding of the many other events and processes that affected the host rocks (Table 1).

The Silurian and Lower Devonian carbonate rocks which host most of the deposit are silty to argillaceous limestones and dolomites, commonly thinly laminated. They were deposited under conditions conducive to the preservation of organic matter (Matti and McKee, 1977). Thrust faulting during the Devonian-Mississippian Antler orogeny resulted in deep burial of these units, to depths locally exceed-

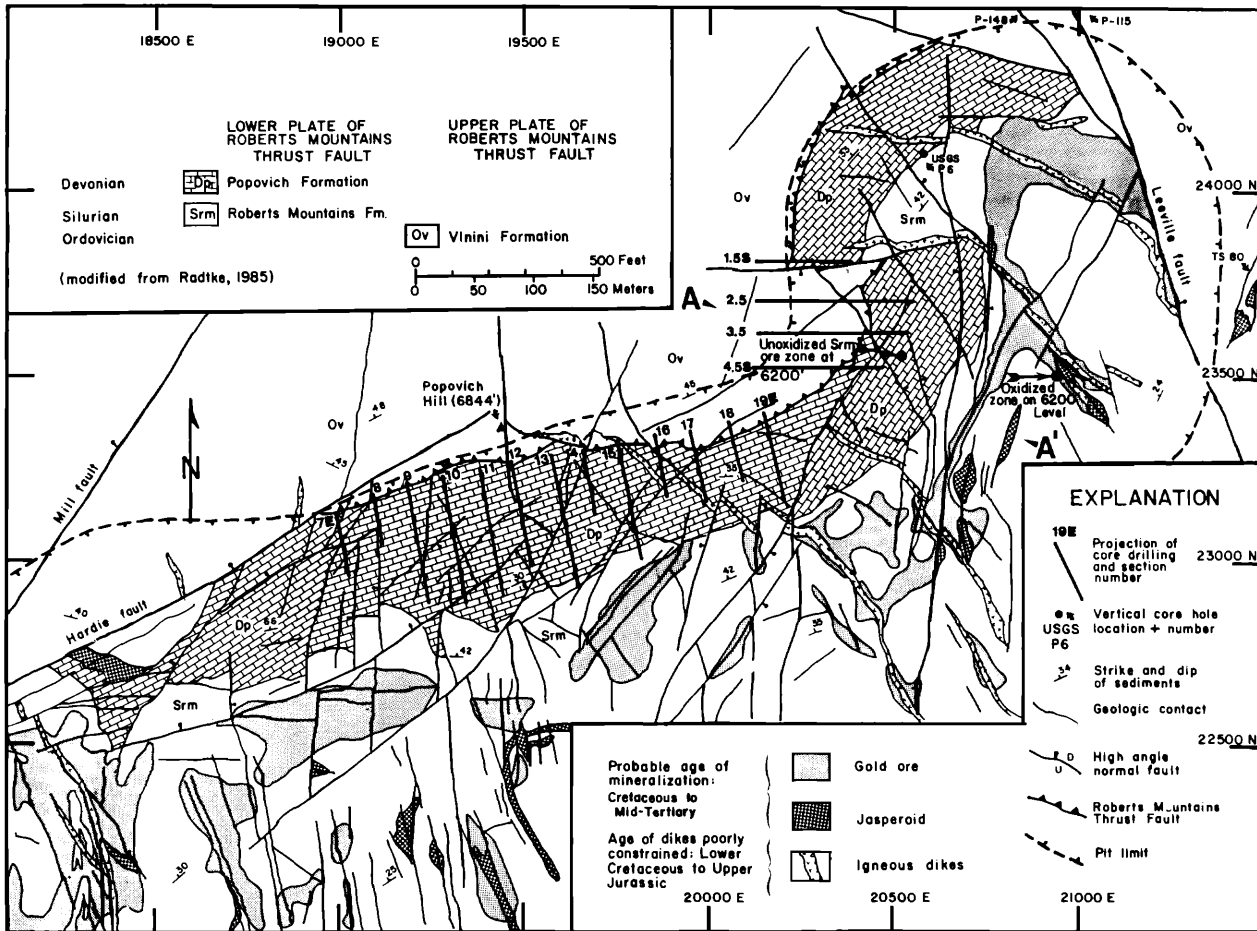


FIG. 2. Generalized geology of the East orebody and vicinity, Carlin gold deposit, showing the projection of underground core drilling and pit exposures described in this study. Geology and ore distribution from Radtke (1985), representing exposures 30 to 90 m above the 1983 to 1985 pit levels. Ore zones represent the updip extensions of mineralization intercepted in the drill array and pit sampling.

ing 5 km (Madrid, 1987). Petroleum generation and migration occurred under these deep burial conditions (Kuehn, 1989; Kuehn et al., in prep.).

Deformation during Late Triassic to Late Jurassic time developed the northwest-trending Tuscarora anticline (Madrid and Bagby, 1986; Madrid, 1987). Early Cretaceous igneous activity along this anticline is represented by several granodioritic intrusions, some of which show considerable contact metamorphic effects (Evans, 1974a and b). The Goldstrike intrusion located about 10 km northwest of the Carlin mine has been dated at 121 Ma (Hausen, 1967), though Arehart et al. (1989) find ages as great as 160 Ma. Spatially associated with this intrusion are numerous Au orebodies including the Bluestar, Genesis, Bazza, Long Lac, Northstar No. 9, Post, Lower Post, Betze, Purple Vein, Deep Star, and Screamer de-

posits (Christensen et al., 1987; Sheppard and Zimmerman, 1988; Bettles, 1989; Knutsen et al., 1991).

Pre-Basin and Range extension in north-central Nevada began around 37 Ma during the earliest Oligocene (Regnier, 1960; Zoback et al., 1981) and coincided with a second period of intrusive activity in the Carlin trend marked by small plutons, stocks, and a districtwide series of dikes of intermediate composition (Silberman and McKee, 1971; Evans, 1980). Major extensional faulting and basin-range structure commenced about 17 Ma and was followed by a third period of igneous activity in the mid-Miocene around 14 Ma marked by rhyodacitic flows and domes exposed on the western flank of the Tuscarora range (McKee et al., 1971; Radtke et al., 1980).

Most previous workers have proposed a late Tertiary age for Au deposition at Carlin on the premise

TABLE 1. Generalized Sequence of Events in the Carlin District

Age	Event no.	Events
Siluro-Devonian	1	Deposition of Roberts Mountains Formation + western assemblage rocks
Late Devonian to Early Mississippian	2	Burial and diagenesis
	3A	Antler orogeny and deep burial under Roberts Mountains allochthon
	3B	Hydrocarbon generation-migration
Late Triassic to Late Jurassic	4A	Folding and development of the Tuscarora anticline
	5A	Districtwide granodioritic intrusive activity
	5B	Early barite $\pm$ base metal veins (could possibly be older features)
Late Jurassic to Early Cretaceous	5C	Maturation of hydrocarbon to pyrobitumen and CH <sub>4</sub> gas production
	5D	Earliest possible date of Au mineralization is around 120 Ma
42 to 37 Ma	6	Prebasin and range extension erosion?
Latest Eocene to earliest Oligocene	7	Districtwide igneous dikes and minor intrusions of intermediate composition
	8	Minimum age, Au mineralization and alteration
Beginning around 17 Ma	9	Very active basin and range faulting with extensive erosion and uplift
Mid-Miocene around 14.4 Ma	10	Igneous activity (rhyodacitic and rhyolitic flows and domes)
Pliocene	11	Lake beds with mineralized cobbles of silicified jasperoid material
Recent	12	Surficial weathering and oxidation

that basin and range faults served as hydrothermal fluid conduits (Hausen and Kerr, 1968; Radtke et al., 1980; Radtke, 1985; Rye, 1985). Formation of the Carlin deposit is constrained to be later than Late Jurassic to Early Cretaceous and earlier than Pliocene in age by the following facts: (1) contact-metamorphic calc-silicates in the Goldstrike area are altered and locally mineralized along with adjacent granodiorite (Morrow and Bettles, 1982; Sheppard and Zimmerman, 1988; Arehart et al., 1989; Bettles, 1989), and (2) clasts of Au-bearing jasperoid are entrained in the Pliocene Carlin Formation (Rota, 1987; Rota and Ekburg, 1988). Several additional observations suggest that mineralization is older than 14 Ma (mid-Miocene). The silicic 14 Ma volcanic rocks are not altered or mineralized and lie unconfor-

mably on the Au-bearing rocks. Structural studies by Bakken and Einaudi (1986) show that north-northeast-trending basin-range structures commonly are barren and postdate Au mineralization. Moreover, crosscutting relations at the Carlin mine allow mineralization to be as old as Early Cretaceous (120 Ma). Arehart et al. (1989) find ages between 40 and 148 Ma for alteration silicates at the Post deposit. O. D. Christensen (pers. commun., 1991) suggests that multiple ages of Au mineralization may exist; however, the uniformity of alteration suggests that a single major episode is represented. The unconformable relations of the 14 Ma volcanic rocks over the mineralized rocks indicate that the present surface has been in the near-surface environment since the mid-Miocene, and therefore, deposits exposed in the Carlin trend may have had a long history of supergene alteration and weathering.

#### Characteristics of host rocks

Silty carbonate rock in the upper 250 to 300 m of the Silurian Roberts Mountains Formation is the major host for Au ore at the Carlin deposit. Detailed petrographic and mineralogic studies of 246 samples of the Roberts Mountains Formation throughout north-central Nevada (Mullens, 1979, 1980) show the typical initial mineralogy of the upper laminated Roberts Mountains unit to be 30 to 50 percent calcite (by volume), 15 to 35 percent dolomite, 20 to 30 percent quartz silt, 5 to 15 percent illite, 2 to 4 percent K feldspar silt, 0.2 to 1.0 percent pyrite, and 0.2 to 0.45 percent organic matter. In addition, minute stringers and blebs of secondary (epigenetic) quartz were observed in some samples, and minor chlorite was detected in about one-fourth of the samples studied by Mullens (1980). Traces of heavy minerals and minor kaolinite were also noted.

Three main types of beds can be texturally distinguished in the upper Roberts Mountains Formation: (1) laminated argillaceous dolomitic limestones with interbedded calcareous siltstones, (2) relatively massive carbonate beds, and (3) medium- to coarse-grained carbonates comprised largely of bioclastic debris. Planar depositional fabric oriented parallel to stratification (lamination) results in centimeter-thick, platy, argillaceous carbonate, or laminated beds. The interbedded coarser grained calcareous siltstones, generally <2 cm thick, contain more quartz silt and less clay than adjacent laminated beds (Fig. 3).

In the immediate area of the Carlin deposit the upper 100 m of the Roberts Mountains Formation contains a few percent of the third distinct lithotype mentioned above: coarser clastic fossil-rich calcareous grainstones and packstones that range in thickness from <0.25 to >50 cm. These bioclastic interbeds are lenticular and gradually thin and pinch

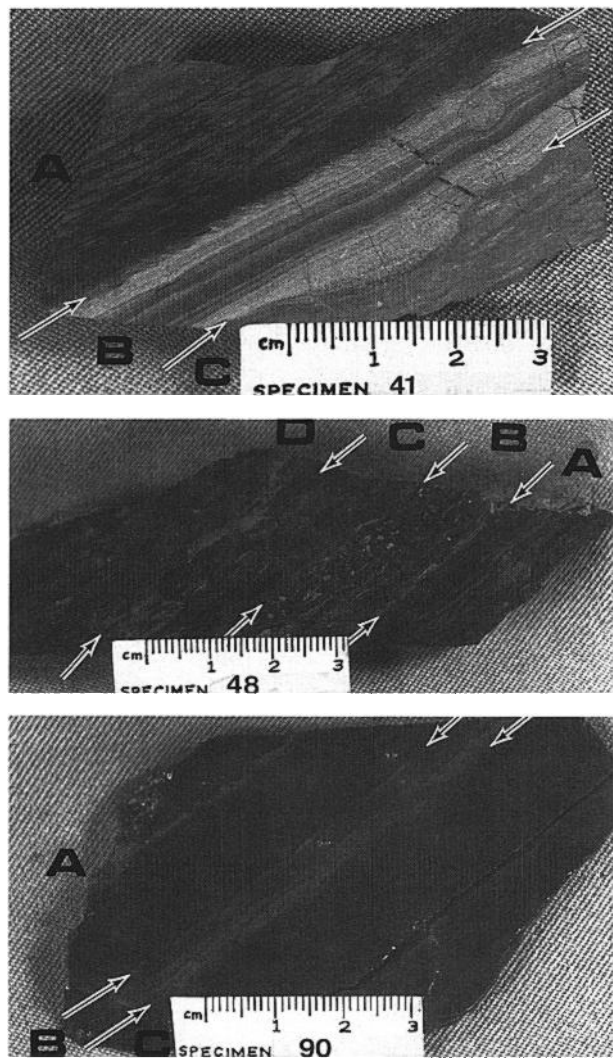


FIG. 3. Unoxidized Roberts Mountains Formation samples from section 15E. For chemical analyses see Table 2. Sample 41 is very mildly leached, 41-B is a calcareous siltstone interbed, and bed 41-A shows numerous elliptical peloids typical of laminated rocks near the Popovitch Formation-Roberts Mountains Formation contact. Small gash fractures restricted to the silty interbed 41-B contain early hydrocarbon stage calcite and pyrobitumen. Sample 48 is virtually unaltered and chemically similar to background dolomitic carbonates; however, 48-B, a calcareous bioclastic horizon, is distinctly pyritized. Beds 48-B and 41-B show higher amounts of dispersed cubic and framboidal pyrite as well as  $\text{SiO}_2$  and  $\text{FeS}_2$  replacement of fossil hash. Sample 90 is moderately acid leached and contains a 0.5-cm-thick porous dolomitic siltstone horizon in typical laminated unoxidized ore.

out into laminated beds; they have lateral extents ranging from several meters for thin beds to >150 m for thick beds. Clastic constituents are typically sand and granule sized; however, recognizable crinoidal columnals and coral, brachiopod, and bryozoan fragments, as well as carbonate mudstone intraclasts, also occur in these bioclastic horizons (Fig. 3, specimen

48, bed B). Commonly, within the Carlin deposit these better sorted bioclastic interbeds, as well as interbedded coarser grained calcareous siltstone horizons, were selectively leached, brecciated, and replaced by silica. These coarser clastic beds apparently were important stratiform conduits for hydrothermal fluids as a consequence of having higher inherent permeabilities than adjacent laminated beds.

Numerous severely altered, premineralization dikes are located within the Carlin deposit and immediate vicinity. These dikes are of intermediate composition and have been described as biotite-rich granodiorites and/or dacites (Hausen and Kerr, 1968; Radtke, 1985). Compositional and textural variations suggest that more than one type of dike may exist within the mine; however, severe alteration has hampered precise radiometric age determinations and limited petrographic or chemical studies. No crosscutting relationships between dikes of different varieties have been documented at Carlin. Dikes altered and cut by Au mineralization commonly constitute Au ore; however, the same dike is barren of Au above and below the orebody. Dikes commonly occupy north-northwest-trending structures and are cut by east-west- and north-northeast-trending faults (Fig. 2). Intense shearing suggests that in many cases movement continued along north-northwest structures after dike emplacement.

#### *Orebody geometry and first-order controls*

Gold mineralization at the Carlin deposit is semi-conformable within the upper Roberts Mountains Formation along a strike length of around 2,100 m; it dips approximately  $30^\circ$  NNW underneath Popovich Hill. As shown in Figure 2, a series of near-vertical east-northeast- and north-northwest-striking normal structures served as local fluid conduits and also strongly influenced the overall distribution and geometry of orebodies at Carlin (Radtke, 1985; Bakken and Einaudi, 1986). The combination of these two controls, one stratiform and one structural, results in a series of anastomosing pods and lenses of Au mineralization whose overall geometries or boundaries are determined by a given assay cutoff or scale of observation. At values of 0.5 ppm Au, mineralization is fairly continuous over 2 km of strike.

The Carlin mine area has been divided into four orebodies: East, Main, South Extension, and West (Radtke, 1985) largely as a function of pit design; however, these four areas also possibly represent separate loci of fluid influx (Fig. 1).

#### *General paragenesis at Carlin, Nevada*

Three major episodes of element mobilization may be distinguished by processes primarily related to (1)

hydrocarbon maturation, (2) Au ore deposition, and (3) subsequent oxidation (Fig. 4). The early hydrocarbon history is discussed in detail in Kuehn et al. (in prep.), and details of the paragenesis during the Au ore stage are presented by Kuehn (1989). This paper concentrates on the alteration during the second and third episodes. Descriptions of veinlet paragenesis observed in the Main pit at Carlin are also provided by Bakken and Einaudi (1986).

Major throughgoing veins are rare at Carlin, but small discontinuous veins ("veinlets"), typically 0.5 to 5 mm in thickness, are common in many locations and have been used to determine paragenesis, along with other types of relationships (Kuehn, 1989).

Crosscutting relationships and fluid inclusion work (Kuehn et al., in prep.) show that organic metagenesis occurred under P-T conditions of approximately 155° ± 20°C and 0.6 to 1.4 kbars and was wholly or dominantly a preore event unrelated to mineraliza-

tion. Hydrocarbons were emplaced during or after the Late Triassic to Late Jurassic development of the N 35° W structural trend defined by the Tuscarora anticline. Organic maturation culminated during Mesozoic heating by nearby granodioritic intrusions. Redistribution of organic matter during subsequent Au mineralization is restricted to the physical concentration of solid organic carbon by lithologic compaction or to removal by chemical oxidation. Unambiguous evidence for the influx of organic matter with the hydrothermal fluid is lacking.

As a first approximation the numerous veinlet types in the Au orebody can be segregated into main and late stages based on whether or not they cut jasperoids and other intensely silicified, altered, and mineralized rocks that occur in and near the Au orebodies (Fig. 4). Because of coherent spatial associations of Au, As, Sb, and other heavy elements with nearby silicification, as discussed later, it is assumed that Au was introduced at least partly during silicification and development of jasperoids that are spatially related to ore.

Mineralized jasperoid breccias locally contain clasts of altered dike material, entrained sheared barite clasts, and polyolithic, altered rock fragments which are themselves veined and brecciated. The jasperoids in turn are locally cut by milky white quartz veinlets which contain low-salinity, CO<sub>2</sub>-rich fluid inclusions (Kuehn and Rose, 1986, 1987a; Rose and Kuehn, 1987; Kuehn, 1989). Jasperoid breccia zones are commonly rebrecciated and locally contain vuggy tabular crystals of barite, euhedral calcite ± microcrystals of quartz, or are partially recemented by these same minerals. Unoxidized jasperoids also locally contain pods, pockets, and fracture coatings of dickite ± kaolinite, as well as late euhedral vug-filling cinnabar, tetrahedrite, and (rarely) exotic Tl-Sb-As phases (Radtke, 1985). Unoxidized silicified and altered zones also contain late barren white calcite veins and calcite-realgar veins.

OBSERVATION	STAGE	EPISODE
Travertine and hyaline opal Stibnite to stibiconite, native S FeOx and kaolinite on fractures Vug and fracture-fill cc w/FeOx Peach-colored calcite veins Oxidation of pyrite, carbon removal	RECENT TO PRESENT  OXIDATION STAGE: imposed on altered, mineralized and barren rocks	YOUNGEST (3) POST- gold ore
Calcite veinlets; clear euhedral xtls Vug xtls in jasp:barite, cc, quartz Massive white barite w/minor stib Orpiment-cc-barite-realgar-stibnite Calcite-realgar veins: hangingwall Calcite ± Fe-dolomite veinlets  Quartz veinlets w/CO <sub>2</sub> -rich fluid inclusions cut jasperoids and argillically altered dikes  Jasperoid breccias+stockwork vns Large-scale carbonate removal and progressive silicification with local jasperoid formation and extensive dike alteration	LATE ORE STAGE: yet still related to (mineralization in terms of time and process  MAIN ORE STAGE: siliceous replacement of unoxidized rocks	(2) SYN- gold ore
<b>IGNEOUS DIKES CUT CARBON ZONES</b>		
Pyrobitumen veinlets cut early barite - rare last evidence of carbon mobility  Sheared greyish barite veins with minor galena ± sphalerite  White calcite ± euhedral quartz Brecciated pyrobitumen and cc Quartz ± calcite ± pyrobitumen Dark calcite-carbon stylonites  Soft-sediment deformation Synsedimentary features	EARLY BARITE ± BASE METALS  HYDROCARBON STAGE  Depositional and Diagenetic Stages	(1) PRE- gold ore  OLDEST

FIG. 4. Generalized paragenetic sequence of veinlet types and alteration features at the Carlin mine. Late ore-stage features cut altered and mineralized rocks; some may be cotemporal with main-stage features but are located farther from hydrothermal conduits.

### Hydrothermal Alteration Studies

#### Oxidation and bleaching

The conversion of pyrite to Fe oxide and the oxidation of small amounts of organic carbon give rise to the abundant buff-tan rocks which contrast with the gray-black unoxidized rocks seen elsewhere in the mine. Through common usage by numerous workers over the last 20 yr, this simple color contrast is the popularly accepted descriptive definition of oxidized versus unoxidized, reduced rocks in these deposits. Therefore, oxidation hinges largely on pyrite stability and the presence or absence of small amounts of organic carbon (generally <0.2 wt %). Several previous studies have implied that much oxidation occurred as a hypogene process contemporaneous with

acid leaching and later stages of Au mineralization (i.e., Radtke, 1985).

The following observations suggest that oxidation is related to deep weathering rather than hydrothermal processes:

1. At a hand sample or microscopic scale, oxidation initially occurs adjacent to fractures and veinlets (Fig. 5A) or along permeable interbeds (Fig. 5C).

2. Abrupt boundaries between oxidized and unoxidized zones are commonly defined by late hairline calcite veinlets (Fig. 5B and C) which acted as impermeable barriers to the oxidizing fluid. Therefore, oxidation postdates these late-stage calcite veinlets (Fig. 4).

3. The oxidized rocks contain amorphous or goethitic Fe oxide and only rarely hematite, which is

the stable phase at temperatures above about 80°C (Langmuir, 1971). Fe oxide is commonly pseudomorphic after early pyrite (Fig. 5D) and also occurs as fracture coatings with vuggy calcite ± kaolinite. The Fe oxide defining the oxidized rocks is therefore interpreted to have formed during a lower temperature, later episode than the hydrothermal mineralization. Hydration of hematite to goethite is not likely (Langmuir, 1971).

4. At the mine scale, steeply dipping north-northeast faults in unoxidized rocks that show only minor displacement above, within, or below the orebody commonly contain buff-colored oxidized fault gouge which in many cases is still highly calcareous.

5. Deep oxidation, in some cases extending >250 m below the present surface, is preferentially developed downdip along intensely leached, very perme-

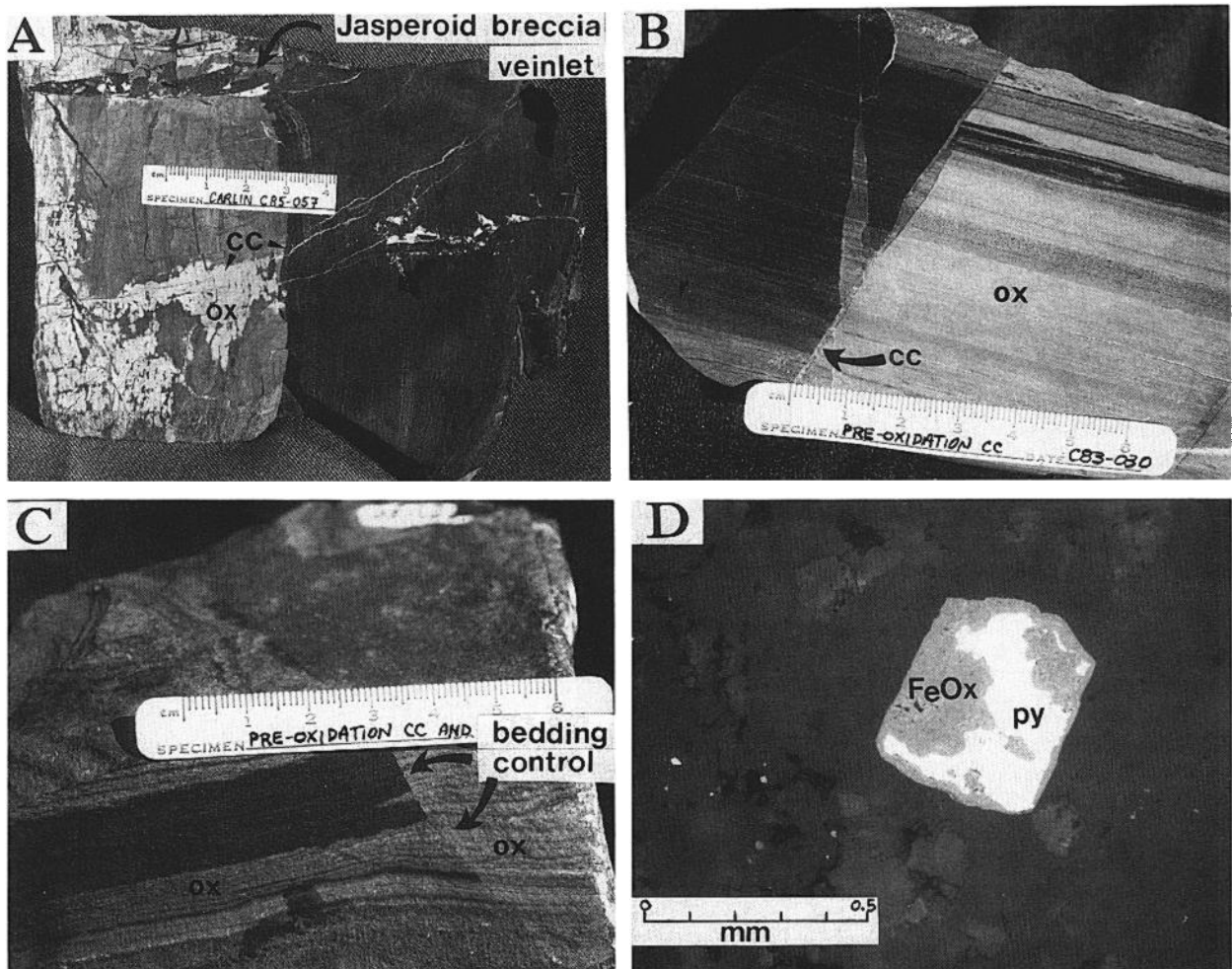


FIG. 5. Typical oxidation features in Carlin ores and country rocks. Cc = calcite, ox = oxidized rock, py = pyrite. A. Selective oxidation away from fracture in a silicified, mineralized sample. Sample C85-057, 6,220-ft level (N23440, E20115). B. Sharp contacts between oxidized and unoxidized rock along hairline-thin, late-stage calcite veinlets. Sample C83-030. C. Fine-scale oxidation controlled by permeability variations along bedding as well as late-stage calcite veinlets. D. Pseudomorphic replacement of pyrite by largely amorphous goethitic and limonitic Fe oxides.

able footwall beds; however, it also extends into adjacent, less altered calcareous zones.

6. Versions of all alteration and mineralization features, including bedded jasperoids, jasperoid breccias, and leached decarbonated rocks, can be identified in both the oxidized and unoxidized zone, with consistent mineralogical effects and only minor changes in major element chemistry.

7. Dickite, a high-temperature polymorph of kaolinite (Lovering, 1949), occurs along fractures and in porous unoxidized jasperoid interbeds, indicating that argillization, as well as leaching and silicification, is not necessarily synonymous with oxidation.

8. At the district scale, the bulk of the Au mineralization in the Carlin trend, especially in the deeper deposits in the Goldstrike area, is unoxidized and contains pyrite and/or marcasite (Bettles, 1989).

These observations show that oxidation at the Carlin deposit is a product of deep weathering and is not related to hydrothermal mineralization. Previous work by Bakken and Einaudi (1986) supports this interpretation. Geologic relationships in the southern portion of the Carlin trend and K-Ar studies on alunite suggest that extensive deep weathering may be as old as mid-Miocene (W. C. Bagby, pers. commun., 1986; Arehart et al., 1991; B. J. Maher, pers. commun., 1991).

Studies of the electrochemistry of coal slurries show that oxidizing agents such as  $\text{Fe}^{+3}$  can oxidize carbon to  $\text{CO}_2$  at room temperature (Dhooge et al., 1982; Dhooge and Park, 1983). Various geophysical methods, such as electrical conductivity and resistance, show that in many cases mature organic matter is a relatively good conductor. Therefore, some deep oxidation at Carlin may be related to electrochemical reactions involving atmospheric oxygen and dissolved iron in shallow ground waters and to the conduction of electrons from depth along carbonaceous horizons. Analogous electrochemical self potentials have been reported from oxidizing massive sulfide orebodies (Sato and Mooney, 1960).

#### *Whole-rock mineralogy*

Silica occurs in several generations and varieties including detrital quartz grains, diagenetic replacements of fossil fragments by chert (Armstrong et al., 1987), authigenic quartz crystals grown during the early hydrocarbon stage, and hydrothermal silicification as both euhedral overgrowths on detrital quartz grains and pervasive replacement by silica. Jasperoid commonly shows a very fine grained xenomorphic texture and locally contains dolomite rhombs, pyrite, encapsulated clots of white mica, and organic matter and more rarely remnant blebs of calcite. Quartz veinlets are rare and are most commonly associated with jasperoids and altered dikes. Locally, very late microcrystals of quartz grow along fractures and coat

cavities in altered rocks. Authigenic quartz crystals associated with early hydrocarbon maturation occur in veinlets throughout the mine, both in and out of ore, even in zones which have subsequently been oxidized.

"Sericitic" in this paper refers to hydrothermal K mica formed during the main and late stages of Au mineralization and alteration, as opposed to any indigenous sedimentary or diagenetic K mica, which is termed "illite." Petrographic studies and scanning electron microscopy of unoxidized, mineralized, and altered laminated interbeds show a coarsening and alignment of micaceous material; similar observations are reported by Bakken et al. (1989).

Minor chlorite also occurs in some samples; however, a systematic spatial relationship between chlorite and mineralization is not apparent.

Although montmorillonite is reported to be widespread in the Carlin district (Hausen and Kerr, 1968; Evans, 1980; Radtke et al., 1980; Hausen et al., 1983; Radtke, 1985; Evans and Peterson, 1986; Bakken, 1990), 1.4-nm clays which expand upon glycolation were not found in any of the more than 100 samples selected to represent primary unoxidized alteration and mineralization. XRD studies of clay-rich samples collected during core logging showed the questionable presence of small amounts of montmorillonite only in oxidized altered zones and in fault gouge.

In certain oxidized and unoxidized altered rocks at Carlin, white to gray clay occurs as fracture coatings and/or dusting of shears, bedding surfaces, and fractures. XRD studies of these fracture coatings show the distinct 0.7-nm peak of kaolinite-group minerals. Detailed XRD studies on mineral separates collected from fracture fillings in unoxidized jasperoids show the triplet of minor peaks between 0.444 and 0.427 nm characteristic of dickite, the polymorph of kaolinite commonly associated with argillic alteration in hydrothermal environments (Lovering, 1949). SEM-EDS studies of these fracture fillings revealed well-crystallized hexagonal booklets of Al silicate, commonly  $>100 \mu\text{m}$  in diameter. Dickite was also identified as a common phase in argillically altered dikes at Carlin. During detailed XRD studies I-T kaolinite was also identified both as fracture coatings and in whole rocks.

In general, whole-rock XRD analyses could not clearly distinguish kaolinite-group minerals due to the poor resolution of minor peaks, so in the absence of additional mineral separate data, samples showing a distinct response at 0.7 nm are simply reported as containing kaolinite-dickite.

Several stages of barite mineralization may be distinguished (Fig. 4), including a very early premineralization barite  $\pm$  base metal stage. Although late ore-stage calcite  $\pm$  realgar  $\pm$  barite veins occur as much as 75 m above mineralization, veins containing barite

are not restricted to oxidized or hanging-wall portions of the orebody as reported by Radtke et al. (1980). Barite also occurs in unoxidized mineralized and altered rocks, largely in shear zones and along faults, both within and outside the ore. Where these late-stage veinlets traverse porous, leached, and altered rocks, both barite and calcite typically occupy available void space and locally permeate the rock. These zones are highly anomalous in Ba, As, and Sb and may also contain high Au values. Barite commonly occurs as a tabular vug-filling mineral in silicified jasperoid breccias and as a minor component in more severely leached porous rocks. The intimate association of barite with silicified zones and jasperoids suggests a common heritage of Ba, Au, As, Sb, and  $\text{SiO}_2$ .

#### Zonation of alteration mineralogy

A zoned alteration pattern inferred from core logging plus several detailed studies in unoxidized carbon-bearing rocks is summarized in Figure 6. The mineral assemblages are zoned as follows: (1) unaltered siltstone containing calcite, dolomite, illite, quartz, K feldspar, and pyrite; (1A) unaltered, but with extensive calcite veining; (2) decalcified: minor remnant calcite with dolomite + illite + quartz + pyrite; (3) decarbonated-argillic: minor remnant dolomite with illite-sericite + quartz + pyrite; (4) siliceous-argillic: quartz + illite-sericite + pyrite; and (5) jasperoid: quartz + dickite-kaolinite + pyrite. This typical pattern of alteration zoning can be recognized in essentially all drill holes and in exposures in the open pit (Figs. 7 and 8).

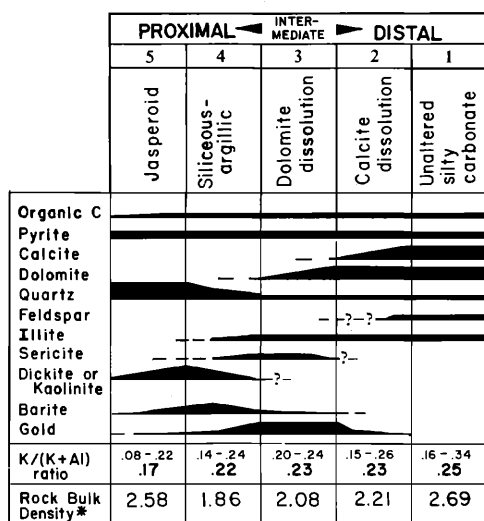


FIG. 6. Zonation of alteration at the Carlin deposit as defined by mineralogical stabilities and spatial relationship to conduits of hydrothermal fluids. K/(K + Al) values from Radtke et al. (1972), Mullens (1979), Radtke (1985), and Kuehn (1989). Bulk densities ( $\text{g}/\text{cm}^3$ ) from Hausen (1967) and Hausen and Kerr (1968).

The terms “proximal” and “distal” used in this paper express proximity to conduits of influx for incoming deep hydrothermal fluid. For example, the proximity of a conduit for the incoming deep hydrothermal fluid is correlated to increased carbonate removal at a given location. This spatial relation is observed regardless of the scale of observation and applies equally to zonation around major feeder structures or around coarser grained, more permeable interbeds serving as stratiform conduits within the upper Roberts Mountains Formation.

Figure 7 illustrates the spatial relationship between Au ore, silicification and decalcification in two unoxidized drill core intercepts, a proximal intercept near a fault inferred to be a conduit of hydrothermal influx (“feeder zone”), and a more distal intercept away from any obvious structures. Note that silicification is absent in distal alteration zones although similar clastic interbeds are intimately associated with mineralized zones in both cases. Calcite veining is a common hanging-wall feature and is also associated with distal ore zones and the footwalls of distal intercepts. Calcite veining is distinctly less common in decarbonated proximal footwall rocks.

The major features of hydrothermal alteration and mineralization at Carlin are shown in a generalized cross section through the East orebody (Fig. 8). Several additional effects are superimposed on this zoned pattern of carbonate removal and  $\text{Al} \pm \text{K}$  silicate alteration: (1) gold deposition, (2) late-stage calcite veining, (3) silicification and jasperoid development, (4) pyritization, (5) barite deposition in vugs, void spaces, and veins along faults and fractures, and lastly, (6) oxidation.

**Gold mineralization:** Gold occupies a range of positions in the alteration zoning, occurring most abundantly in decalcified rocks which still contain appreciable dolomite, as discussed later. Erratic high Au values also occur in intensely decarbonated or silicified rocks and less commonly in calcareous rocks.

**Carbonate dissolution and calcite veining:** Above the ore, mainly in the Popovich Formation, the rocks contain abundant sedimentary calcite plus abundant white calcite veins (Figs. 7 and 8). These hanging-wall calcite veins commonly amount to several percent of the rock and range from micro-sized examples  $<0.2$  mm thick and several centimeters long, to veins  $>10$  cm thick and continuous over tens of meters. In general, calcite veinlets are  $<1.0$  cm wide and better developed in more competent, less argillic interbeds; calcite veinlets usually dip steeply ( $>75^\circ$ ).

With increasing depth, calcite (as indicated by reaction with dilute HCl) in both veinlets and rock decreases and disappears over an interval of a few tens of feet (Fig. 7). These decalcified rocks are typically more porous due to carbonate removal, and noticeably less dense than unaltered rocks (Fig. 6). Petro-

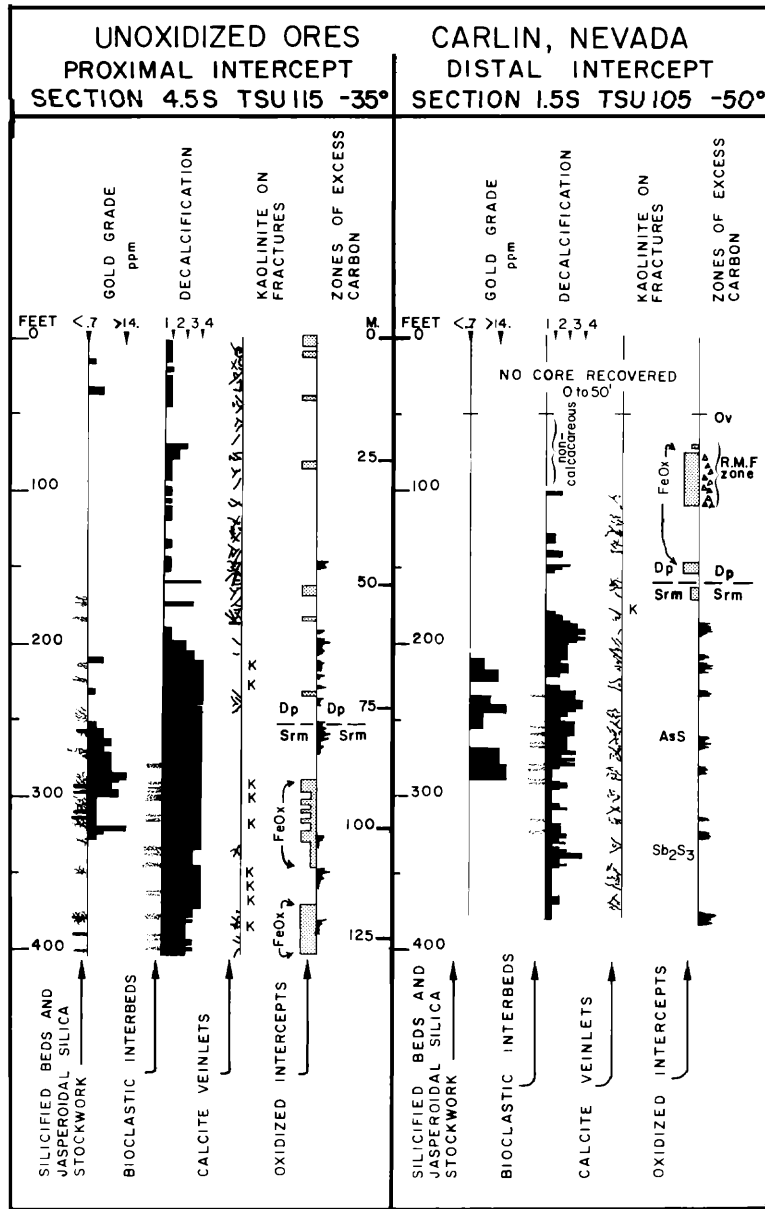


FIG. 7. Spatial relationships between typical proximal and distal alteration features and Au mineralization in unoxidized ore intercepts of drill holes TSU 115 and 105, simplified from logging at a 1:60 scale. See Figure 2 for location of drill sections. Decalcification is based on reaction with dilute HCl: <1 = slightly decalcified or dolomitic, 1 to 2 = mildly decalcified, 2 to 3 = moderately decalcified, 3 to 4 = very slightly calcareous, and >4 = total lack of reaction (but note that dolomite can still be present). "Excess carbon" indicates introduced organic matter and hydrocarbon-stage veining. Dp-Srm = Devonian Popovitch Formation-Silurian Roberts Mountains Formation contact, Ov = Virini Formation, R.M.F. = Roberts Mountains thrust fault, K = kaolinite.

graphic and XRD studies indicate that rocks in the decalcified zone contain dolomite, quartz, illite-sericite, carbonaceous matter, and pyrite. With further depth, and near channels of hydrothermal influx such as faults and permeable interbeds, the dolomite also disappears to leave a very porous, leached, low-density rock composed of quartz, illite-sericite, pyrite,

organic carbon, and locally minor dickite-kaolinite. In zones that were not silicified, these leached rocks have commonly compacted to a laminated shale with very little porosity and permeability.

Beneath the ore zone, large volumes of rock are depleted in carbonate to form a footwall leached zone containing illite-sericite, quartz, pyrite, and

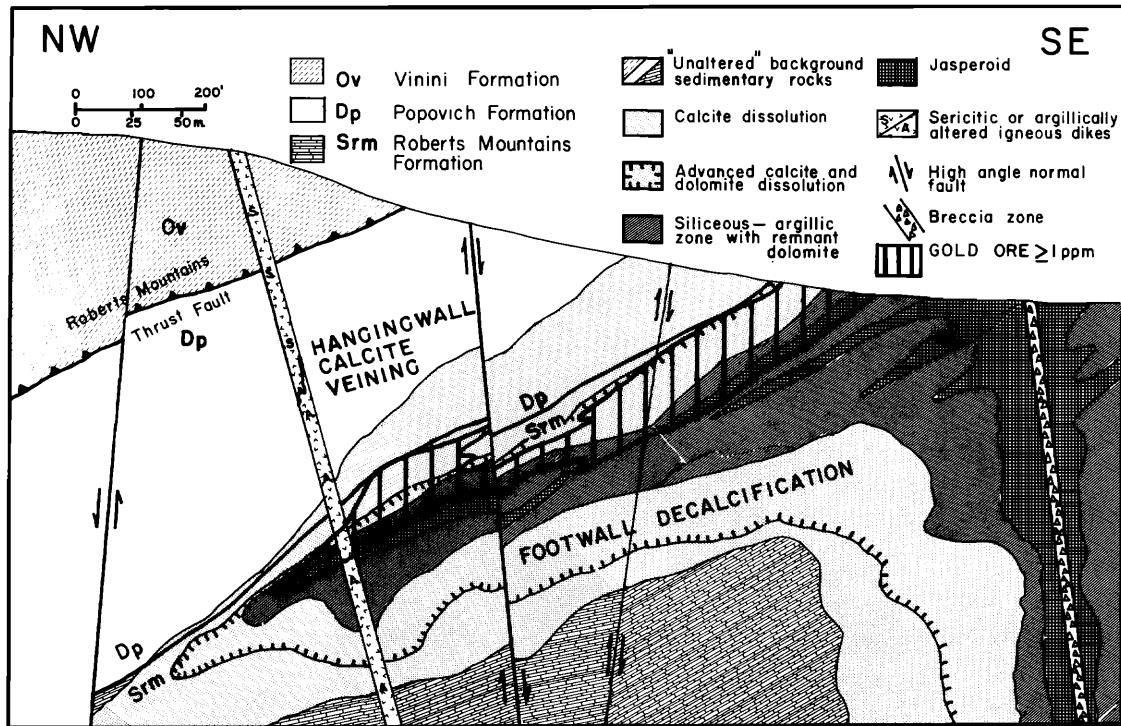


FIG. 8. Schematic composite cross section (approximately A-A in Fig. 2) showing mine-scale spatial relationships of hypogene alteration features and mineralization.

carbonaceous matter (Fig. 7). Judging from exposures south of the mine, carbonate-bearing rocks are present at depth below ore. However, most drill holes, which in some cases extended up to 75 m below the orebody, encountered only dolomite-bearing footwall rocks effectively leached of calcite. Relatively unaltered calcite-bearing footwall rocks were encountered in several holes but were generally restricted to drill holes farthest removed from hydrothermal conduits.

The decalcification alteration is grossly zoned around the entire mineralized volume, but the more intense carbonate removal is zoned around hydrothermal influx channels such as faults, fractures, permeable siltstone interbeds, and bioclastic horizons. Areas of carbonate removal and argillic alteration commonly coalesce and overlap adjacent to multiple influx channels such as fault zones or stratigraphic intervals with numerous coarse clastic horizons. Thus, at a small scale the geometric relationships are extremely complex, with tongues of locally silicified, argillically altered, decarbonated rock extending along permeable beds 10 m or more into carbonate-bearing rock and common islands of less altered rock surrounded by more intensely altered rock.

Although progressive carbonate removal and the alteration of detrital K feldspar and illite to sericite

and development of dickite-kaolinite appear to be both systematic and sympathetic, the late-stage addition of calcite, and limited transport of Al in the most intensely altered zones, complicates the alteration patterns in detail.

*Jasperoid development and silicification:* Alteration close to influx zones is typically characterized by silicification, with illite-sericite still present in some cases but essentially completely replaced by quartz in the most extreme alteration. Near-influx channels in some rocks comprised mainly of quartz, illite-sericite has been converted to kaolinite-dickite. The presence of remnant encapsulated blebs of carbonate as well as clots of mica suggests that intense silicification may have locally occurred prior to complete carbonate removal and illite destruction. In all cases, silica deposition significantly decreases porosity and increases rock density.

*Proximal alteration features:* At the mine scale, proximal intercepts commonly contain intensely silicified horizons and typically show dickite-kaolinite on shears and fractures in more intensely altered zones (Fig. 7). Severe carbonate removal resulting in very porous leached rock, and in many areas a finely fractured character probably caused by solution collapse, is the most diagnostic feature. Macroscopic or petrographic evidence of calcite veinlets is distinctly lack-

ing throughout large volumes of proximal, intensely leached, laminated footwall rock. However, because calcite veinlets locally crosscut decalcified and silicified ore zones and altered rocks, at least some calcite veins must have formed later than carbonate removal (Fig. 4).

Several detailed studies near silicified feeder structures in the open pit show specific examples of typical features of proximal alteration. In Figure 9, the absence of original calcite in this section is typical of proximal alteration. Selective silicification of individual bioclastic horizons from <2 to over 12 cm in thickness is typical near the base of ore and in footwall rocks immediately below mineralization throughout the mine.

The highest Au concentrations occur above the uppermost silicified horizon (0.8 and 1.2 m in Fig. 9). As clearly shown by samples 1 to 6, the bedded jasperoids typically contain lower Au values than immediately adjacent dolomitic shales and argillaceous carbonates. Dickite occurs along fractures in these unoxidized bedded jasperoids. Petrographic and XRD studies as well as K/(K + Al) corroborate the destruction of illite at the expense of kaolinite-dickite formation (Fig. 9). The intensely silicified interbeds are crosscut by later calcite veins even though they lack matrix carbonate. Tabular late-stage barite also occurs in fractures.

Figure 10 shows oxidized proximal alteration centered around a brecciated and silicified fault zone, 183 m east-southeast of the unoxidized section of Figure 9, containing sheared white barite (lacking base metals) and minor amounts of sheared dike material. Between the 6,200- and 6,240-ft levels this exposure is erratically mineralized; however, a plan view of Au distribution at a higher level (Fig. 2) suggests that this same north-northwest-trending structure served as a hydrothermal conduit. East of the fault zone shown in Figure 10, the upthrown block is intensely leached and bleached gray-white, shows dolomite dissolution and kaolinite-dickite development, and is barren of Au (<0.6 ppm). Calcite is essentially absent throughout this proximal exposure. Distinctly different degrees of leaching and kaolinite development on either side of the fault zone suggest some movement postdates alteration.

Adjacent to the fault zone of Figure 10, bedded silicified coarser silty and bioclastic horizons extend tens of meters away from the silicified fault zone and commonly show lateral zoning through decreased silica contents into porous leached zones, and eventually into dolomitic and/or calcareous stratigraphic equivalents. These silicified horizons (bedded jasperoids) are typically brecciated and show textures interpreted to form by collapse. Because some individual angular fragments are only partially silicified, collapse predates intense silicification. Similarly, because distal nonsilicified examples of collapse breccias with high Au contents can be found, it is clear that in some locations silicification follows decalcification, brecciation, and mineralization.

In the oxidized proximal examples of Figure 10, as for the unoxidized samples of Figure 9, the highest Au content within each closely spaced series of samples is nearly always adjacent to, but not in, intensely silicified zones, and four of the five highest values are outside silicified zones. However, relatively high values do occur in some jasperoids and may represent Au encapsulated by silica, as evidenced by siliceous refractory ore recognized during processing. In general, both bedded and structurally controlled jasperoid zones have lower Au values than immediately ad-

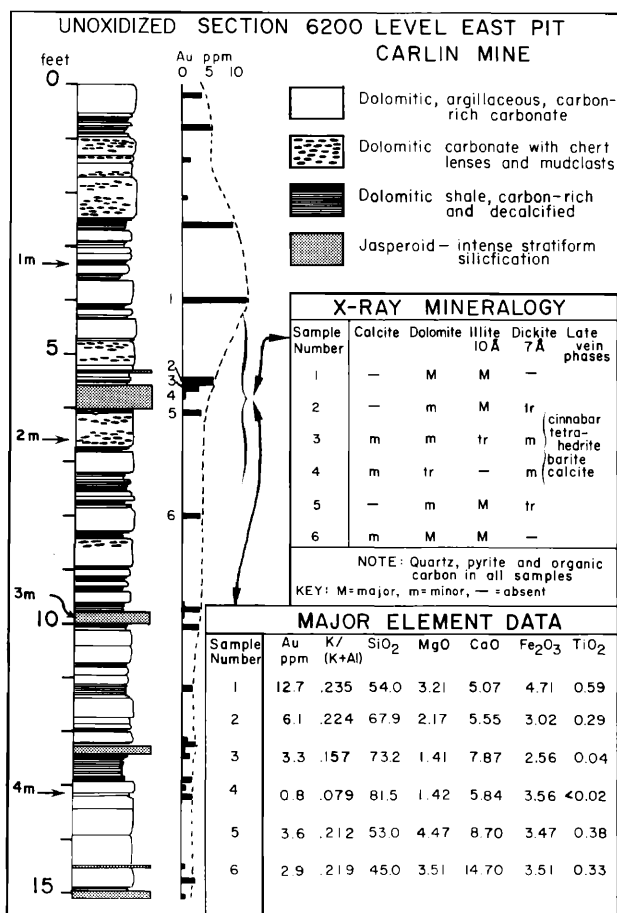


FIG. 9. Proximal alteration near the footwall contact of the unoxidized carbon-rich ore zone on the 6,200-ft level of the East pit (mine coordinates: 23562 N, 20509 E). Bedded jasperoids are selectively silicified coarse clastic interbeds which contain dickite in fractures along with minor vuggy tabular barite as well as rare, euhedral, millimeter-sized cinnabar and tetrahedrite crystals. Late-stage, millimeter-wide calcite + barite veinlets cut the bedded jasperoids. Major Au mineralization develops in the hanging wall above the upper clastic interbeds (feeders) at 1.8 m.

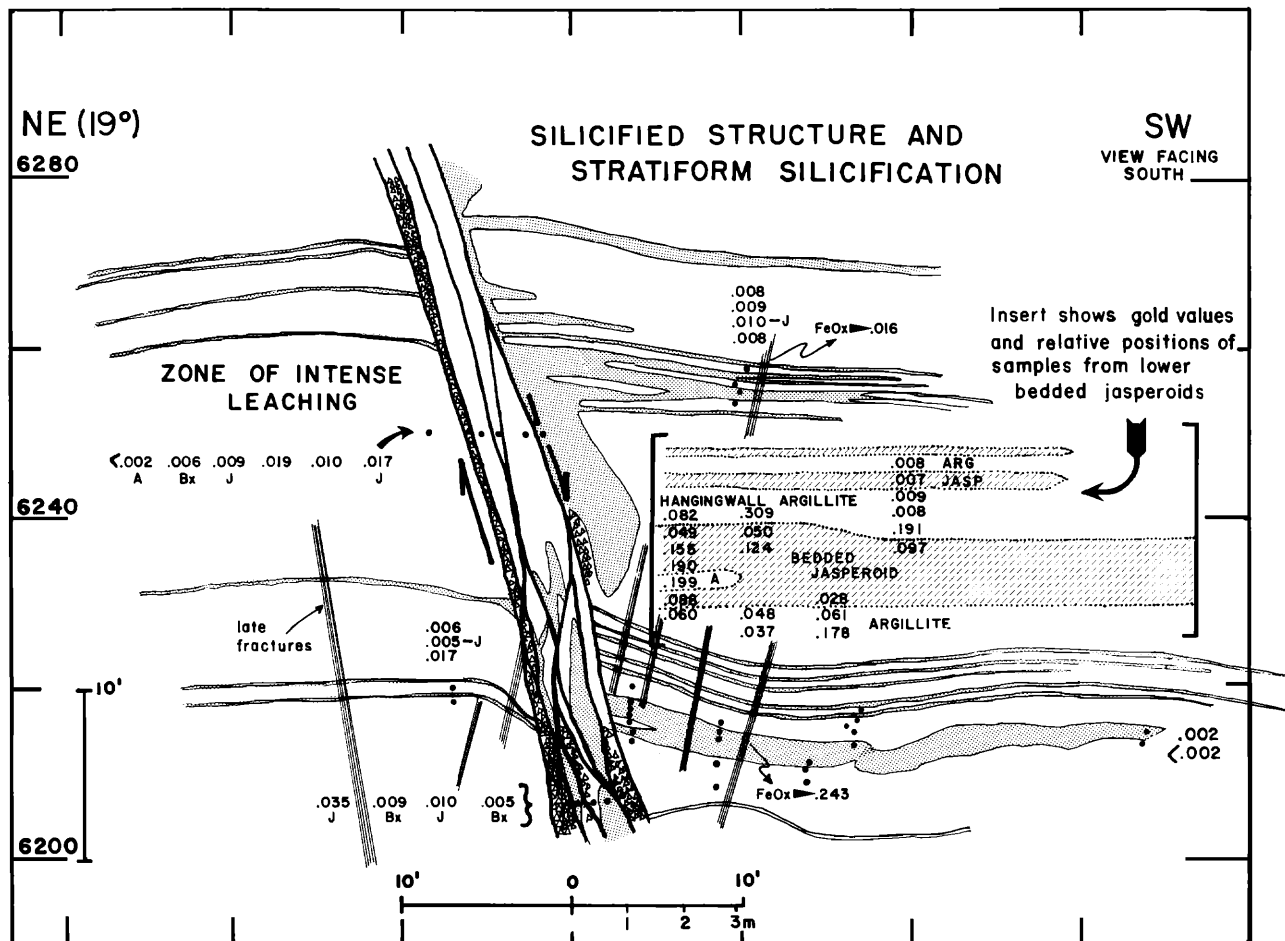


FIG. 10. Oxidized proximal alteration features located in the south wall of the East pit between the 6,200-ft and 6,280-ft levels (coordinates 23503 N, 20958 E, Fig. 2). The fine-stippled pattern along the structure represents hydrothermal silicification (jasperoid) that clearly extends out along selectively silicified interbeds and brecciated bioclastic horizons. Au values in ounces per ton (1.0 opt = 34.285 ppm) are posted in their relative positions near sample locations shown by black dots. Area in brackets is a schematic enlargement of area below to left. A = argillic altered sample, Bx = breccia, J = jasperoid.

adjacent less silicified rocks. Also, in both unoxidized and oxidized cases, the major volume of Au mineralization is located above the strata-bound silicification at the hand specimen, outcrop, and mine scales.

*Distal alteration features:* At mine scale, distal alteration zones are characterized by considerably less carbonate removal, rare macroscopic evidence of kaolinite development, and a general lack of intense silicification. These distal alteration zones typically contain high Au contents (Figs. 7 and 11).

In section 15E (Fig. 11), decalcification shows typical strong stratiform control. Although zones of intense carbonate leaching and Au mineralization are roughly coincident, portions of this distal Au ore intercept are still mildly calcareous. Zones of moderate decalcification or mild leaching contain interbedded calcareous and noncalcareous horizons. Footwall

rocks in section 15E range from strongly calcareous to only mildly decalcified and/or dolomitic, and generally do not show appreciable decreases in density. In this section, oxidation is spatially unrelated to Au ore and is restricted to footwall rocks.

Within 5 m of distal, nonsilicified high-grade carbon ore in section 15E (Fig. 11), individual centimeter-thick beds range from  $<0.17$  to  $>70$  ppm Au and alteration is systematically zoned from relatively unaltered background calcareous and dolomitic carbonates to completely decarbonated rocks (Fig. 12). Within any given hand specimen from three typical examples of unoxidized ore (Fig. 3, Table 2), the coarser clastic units, such as bioclastic horizons or calcareous siltstones, generally contain lower Au contents than adjacent laminated argillic beds. This relationship is analogous to the lower Au contents in

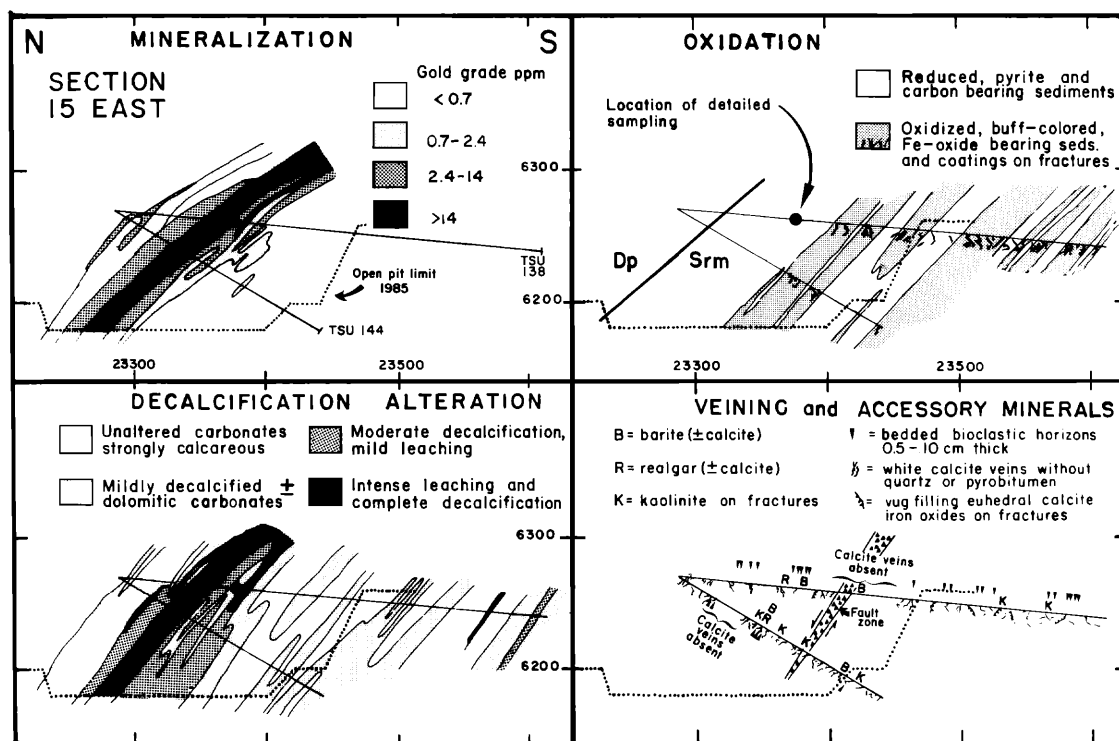


FIG. 11. Distal mineralization and alteration features in unoxidized ore intercept and adjacent rocks, section 15E (drill collars at 23313 N, 19754 E, azimuth 168°, Fig. 2). Footwall rocks show calcite veining and only mild decalcification in both unoxidized and oxidized rocks. For detailed sampling of hole TSU 138 (64' at 14 ppm) see Table 2 and Figure 12.

selectively silicified beds found in proximal alteration zones. The coarser grained interbeds generally contain kaolinite-dickite and lower K/(K + Al) ratios than the adjacent laminated beds, indicating illite breakdown.

In the most distal mineralized zones rare calcite veinlets may persist throughout the ore zone and in footwall rocks (Figs. 7 and 11). Stratiform control is still readily apparent and individual beds range from relatively unaltered calcareous background to intensely decalcified rocks, usually with minor remnant dolomite. Individual beds show mild silicification, but in stark contrast to proximal altered areas, bedded jasperoids are rare. Kaolinite is present locally; however, X-ray analyses are generally required for detection. Coarser grained calcareous siltstone beds and bioclastic horizons are also pyritized in some cases. Distal alteration zones commonly show minor

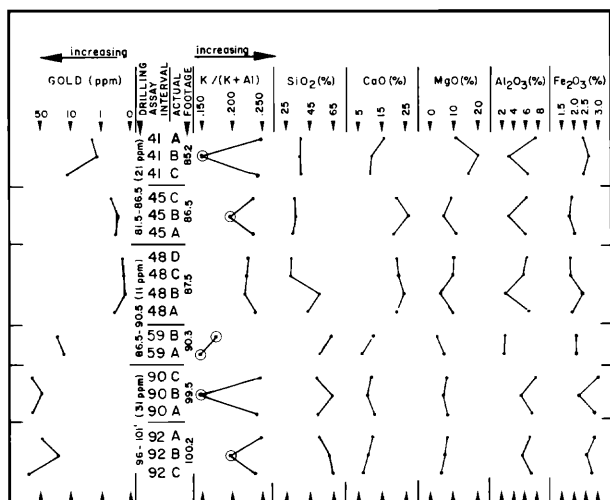


FIG. 12. Major element and Au relations in selected sets of unoxidized distal silicified silty or bioclastic beds and adjacent laminated beds in drill hole TSU-115. This core assayed from 11.3 to 30.9 ppm Au in 5-ft drill intervals; however, individual beds analyzed in this study range from several hundred ppb to >70 ppm. Circled K/(K + Al) values indicate a strong XRD peak for kaolinite-dickite. Adjacent laminated beds generally lacked kaolinite-dickite and contained illite-sericite. At hand specimen scale (Fig. 3), the coarser grained silty or bioclastic interbeds (labeled "B") contain less Au and distinctly lower K/(K + Al) than adjacent laminated beds.

TABLE 2. Chemical Data for Three Unoxidized and Mineralized Roberts Mountains Formation Samples from Section 15E (shown in Fig. 3)

Sample no.	Au	SiO <sub>2</sub>	Al <sub>2</sub> O <sub>3</sub>	K <sub>2</sub> O	TiO <sub>2</sub>	Fe <sub>2</sub> O <sub>3</sub>	MgO	CaO	MnO	SiO	BaO	P <sub>2</sub> O <sub>5</sub>	SO <sub>3</sub>	CO <sub>2</sub>	C <sub>organic</sub>	Total	As	Sb
41A	2.77	37.0	7.56	2.43	0.39	2.39	10.3	15.6	0.028	0.02	0.02	0.15	1.9	21.9	0.83	100.5	167	5
41B	1.75	35.7	3.01	0.51	0.14	2.58	10.4	20.0	0.026	0.02	0.06	0.08	2.8	26.7	0.27	102.3	230	3
41C	14.8	38.4	6.12	1.91	0.33	2.43	9.94	16.2	0.026	0.02	0.02	0.17	2.8	22.5	0.61	101.5	689	19
48A	0.24	32.8	6.43	1.95	0.29	1.93	9.0	21.2	0.024	0.03	0.03	0.11	1.6	25.5	0.34	101.2	116	1.8
48B	0.19	43.1	2.07	0.57	0.09	2.29	4.23	23.6	0.016	0.04	0.01	0.10	3.2	22.8	0.15	102.3	159	2.5
48C	0.22	29.2	5.66	1.57	0.28	1.82	9.91	22.7	0.028	0.03	0.03	0.10	1.1	28.3	0.25	100.9	82	2
48D	0.30	29.1	6.10	1.73	0.29	1.82	9.84	22.1	0.028	0.03	0.03	0.12	2.4	27.7	0.26	101.5	76	1.6
90A	61	51.4	6.58	2.02	0.33	2.81	6.75	9.97	0.013	0.01	0.03	0.14	3.7	13.4	1.48	98.6	2,490	227
90B	50	62.2	5.02	0.83	0.17	2.16	6.22	9.17	0.010	NA	0.05	NA	NA	12.8	0.45	101.6	2,500	117
90C	64	49.5	7.28	2.32	0.39	2.97	7.09	10.4	0.014	0.01	0.02	0.13	3.9	13.9	1.29	99.2	2,710	225

Note that coarser siltstone and/or bioclastic interbeds labeled "B" are usually less mineralized and more altered than immediate hanging and footwall laminated argillaceous carbonates; samples were split into beds along sedimentological breaks and analyzed individually in order to evaluate bedding-scale controls and variance at the hand sample scale; refer to Kuehn (1989) for additional samples and data; Na<sub>2</sub>O values were <0.10 in all samples; Au, As, and Sb in ppm, all others in weight percent, NA = not analyzed

Sample description: 41, very mildly leached dolomitic carbonate; 41A, laminated peloidal calcareous shale, hanging wall to silty horizon; 41B, calcareous siltstone, pyritic with minor hairline calcite veins; 41C, calcareous shale without peloids, beneath silty horizon; 48, calcareous sample very similar to background carbonates; 48A, laminated dark gray peloidal calc-arenite; 48B, calcareous bioclastic horizon with pyritized fossil fragments; 48C, mottled medium to light gray calcareous shale; 48D, mottled dark gray calcareous shale; 90, moderately leached dolomitic carbonate; 90A, laminated very dark gray to black argillic shale with minor silty interbed; 90B, leached, light gray dolomitic siltstone with dusting of kaolinite; 90C, laminated very dark gray to black argillic shale

calcite dissolution at grain boundaries compared to unaltered carbonates.

*Alteration in igneous rocks:* Dikes have also been severely altered, and in some cases, mineralized. Feldspar and mica are converted to dickite-kaolinite in areas of intense alteration, often in the same zones where the adjacent sediments have been silicified, argillized, and mineralized. In more distal exposures (Fig. 8), feldspar and other K ± Al-bearing phases in the dikes are altered to finely intergrown masses of white K mica (sericite) and bright green chlorite. Both the kaolinitized and sericitized dikes are pyritized, and the latter locally contain pyrite pseudomorphs after Fe-bearing silicates such as biotite and hornblende. Marcasite partially converted to pyrite along <101> crystallographic twinning planes has been identified in one altered and mineralized dike sample from the East pit.

Radtke (1985) reports limited and local peripheral alteration of biotite to chlorite and hornblende to epidote in the least altered dikes in the Carlin deposit. This transformation may represent propylitic alteration distal to the kaolinite-dickite and sericitic zones or earlier, very weak, deuteric alteration as originally suggested by Radtke (1985).

A mica-rich mineral separate from a dike in the East pit was dated by the <sup>40</sup>Ar/<sup>39</sup>Ar technique (L. Snee, writ. commun.; Kuehn, 1989, appendix F). This sample contained clots of intergrown white mica and chlorite pseudomorphic after biotite. Plateau ages of 120 ± 1 and 123 ± 1 Ma were obtained on duplicate analyses and showed only minimal resetting to a younger age. A similar age of 111 Ma was obtained by Arehart et al. (1989) for sericite in igneous rocks at the nearby Post deposit. These results seem to indicate an Early Cretaceous age for the formation of the Carlin deposit, though the suggestion of districtwide alteration associated with granodiorite emplacement (Radtke, 1985) cannot be conclusively rejected.

### Major Element Chemical Effects

#### *Volume changes and chemical additions and depletions*

The dissolution of 30 to 50 percent calcite and 15 to 35 percent dolomite from the rocks in and adjacent to the ore zone had significant effects on rock density, strength, and volume. Evidence for significant volume decrease is widespread at both mine and hand specimen scales. For example, bedded sedimentary breccias which show collapse and subsequent mild silicification are associated with stratigraphic intervals immediately beneath high-grade mineralization. Calcite veinlets and microfaults in the hanging wall commonly show slight normal displacement, and both the ore zone and the hanging wall are intensely

broken and sheared as a result of structural readjustments. Many normal faults and pervasive extensional fractures could have developed in response to removal of underlying support by widespread carbonate leaching in the footwall and ore zone (Fig. 8). Quantitative geologic and petrographic evidence for compaction in altered and mineralized rocks at Carlin has been well documented by Bakken (1990). Evidence includes change in thickness of altered vs. unaltered beds, collapse breccias, changes in abundances of quartz and fossil fragments, and flattening of fossil fragments and worm burrows.

In addition, abundant  $\text{CO}_2$ -rich inclusions in certain quartz veinlets indicate the likelihood of  $\text{CO}_2$ - $\text{H}_2\text{O}$  phase separation during mineralization, with accompanying volume increase (Kuehn and Rose, 1987b; Kuehn, 1989). Dilatation of the ore zone due to two-phase separation and high  $\text{CO}_2$  pressures associated with Au deposition also may have allowed for postalteration collapse.

Radtke (1985) argues for the introduction of  $\text{SiO}_2$ ,  $\text{Al}_2\text{O}_3$ ,  $\text{K}_2\text{O}$ , and  $\text{TiO}_2$  by assuming constant volume

and comparing major element contents of unmineralized rocks and unoxidized ores in  $\text{mg}/\text{cm}^3$ , justified by unspecified petrographic evidence (Radtke et al., 1980, fig. 5, p. 653). If any local volume loss due to compaction during or after mineralization has occurred, indigenous, less chemically mobile components would show an apparent increase in concentration. Therefore, alternative methods of evaluating chemical changes are needed.

#### Relative chemical effects using ratios

Local volume changes resulting from postalteration lithologic compaction would have no effects on ratios of chemical components. For example,  $\text{Ti}/\text{Al}$ ,  $\text{K}/\text{Al}$ ,  $\text{Si}/\text{Al}$ , and  $\text{Fe}/\text{Al}$  show the relationships between the relatively immobile component  $\text{Al}_2\text{O}_3$  and other elements which may have been introduced or depleted during alteration at Carlin.

The above chemical ratios in background, altered, and mineralized Roberts Mountains Formation and Dp samples of several types are shown in Figure 13. Background samples are fresh, barren, unaltered

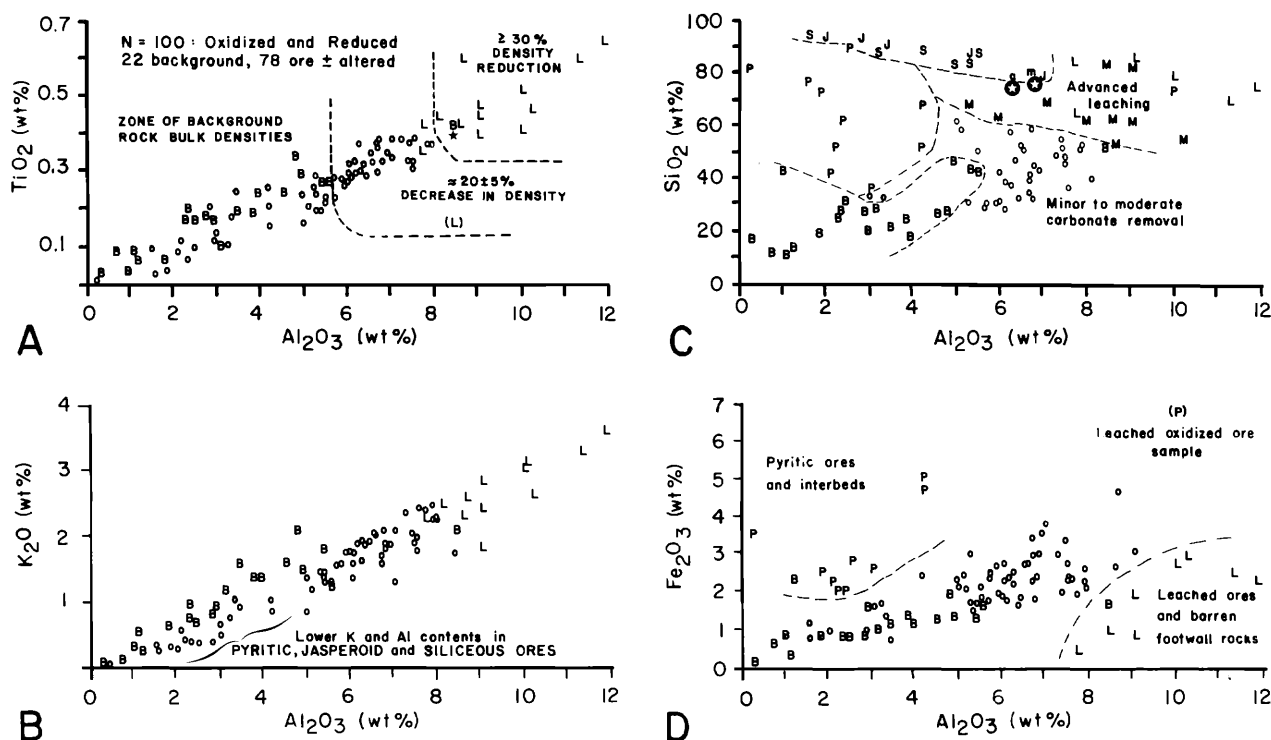


FIG. 13. Plots of Ti, K, Si, and Fe vs. Al for 78 mineralized and altered, oxidized, and unoxidized rocks at the Carlin deposit, and 22 background samples within the district. Approximate boundaries for bulk densities based on data in Hausen (1967). B = background samples, J = barren jasperoids, L = leached barren footwall rocks and leached ores including unoxidized samples, M = leached, proximal ores, o = all other ore types described by Radtke et al. (1980) including "normal," "arsenical," and "carbonaceous," P = pyritic ores and interbeds, and S = siliceous ore. Starred points "a" and "m" in C are average and median values for deep reduced ores (Radtke et al., 1972). Other data sources: Hausen and Kerr (1968), Mullens (1979), and Kuehn (1989).

TABLE 3. Chemical Analyses of Representative Altered and Mineralized Samples from the Carlin Mine

Sample no. and drill hole footage or number	Oxidation state	Au ppm	SiO <sub>2</sub> wt %	Al <sub>2</sub> O <sub>3</sub> wt %	K <sub>2</sub> O wt %	K/K + Al molar ratio		TiO <sub>2</sub> wt %	Fe <sub>2</sub> O <sub>3</sub> wt %	MgO wt %	CaO wt %	MnO wt %	BaO wt %	P <sub>2</sub> O <sub>5</sub> wt %	SO <sub>3</sub> wt %	CO <sub>2</sub> wt %	C <sub>organic</sub> wt %	Total wt %	As ppm	Sb ppm	Tl ppm	Hg ppb
						K	Al															
T14-368.2	Oxidized	0.003	79.3	10.0	3.03	0.237	0.237	0.51	2.70	1.30	0.19	0.006	0.02	0.11	0.1	<0.1	0.13	97.4	1407	148	4	>5000
T14-338.0	Unoxidized	0.003	74.4	11.9	3.60	0.237	0.237	0.64	2.32	1.52	0.18	0.008	0.03	0.15	3.1	<0.1	0.58	98.4	794	28	5	1550
P48-750	Unoxidized	0.015	64.2	7.73	2.41	0.242	0.242	0.42	1.96	4.34	5.55	0.013	0.03	0.13	2.9	8.13	0.49	98.3	240	58	7	4000
P48-783	Unoxidized	0.003	69.7	11.3	3.32	0.232	0.232	0.59	2.46	2.52	2.48	0.008	0.04	0.11	3.9	3.22	0.53	100.2	397	38	5	2150
T07-473.2	Oxidized	0.003	58.9	6.72	2.07	0.242	0.242	0.39	1.84	6.69	9.40	0.034	0.01	0.11	4.2	13.3	0.06	99.5	635	57	79	3250
T07-469.5	Unoxidized	0.005	51.0	7.89	2.45	0.240	0.240	0.37	2.63	7.09	9.79	0.019	0.26	0.15	0.1	13.8	1.53	101.2	964	65	48	>5000
C84-057	Unoxidized	0.580	76.7	1.53	0.32	0.177	0.177	0.09	1.18	3.89	6.54	0.200	0.04	0.19	1.3	8.35	0.01	100.1	104	3	3	2650
T06-458.2	Unoxidized	36	83.8	4.95	1.40	0.225	0.225	0.24	2.39	0.48	0.23	<0.10	0.01	0.15	3.7	0.02	0.19	98.26	4500	440	160	>5000
T06-419.0	Unoxidized	11	88.8	3.18	0.81	0.207	0.207	0.11	1.70	0.25	1.07	<0.10	0.01	0.40	0.3	1.33	1.25	99.54	528	19	22	>5000
T38-#92A	Unoxidized	49	51.7	6.54	2.07	0.245	0.245	0.35	2.75	7.11	10.2	0.013	0.02	0.17	3.5	14.0	1.26	99.7	2440	219	NA	NA
T38-#92B	Unoxidized	31	59.9	5.12	1.20	0.194	0.194	0.21	2.47	6.05	9.20	0.009	0.02	0.11	3.5	12.3	0.97	101.0	1550	138	NA	NA
T38-#92C	Unoxidized	70	62.6	5.84	1.73	0.233	0.233	0.28	2.73	4.92	7.04	0.011	0.02	0.18	3.9	9.31	0.93	99.5	3170	324	NA	NA

SiO values = <0.01 and Na<sub>2</sub>O values = <0.10 in all samples; Au, As, Sb, Tl, and Hg in ppm; all others in weight percent

Sample description: T14-368.2, intensely leached footwall; T14-338.0, intensely leached footwall; P48-750, moderately leached footwall; P48-783, moderately leached footwall; T07-473.2, mildly leached footwall; T07-469.5, mildly leached footwall; C84-057, barren jasperoid—SiO<sub>2</sub> replaced laminated carbonate with pyrite; T06-458.2, siliceous mineralized jasperoid near dike contact; T06-419.0, unoxidized siliceous argillite ore, low-density rock; T38-#92A, laminated hanging-wall dolomitic siltstone from ore section 15E; T38-#92B, moderately leached dolomitic siltstone interbed section 15E; T38-#92C, laminated footwall dolomitic siltstone from section 15E.

rocks and include the data of Mullens (1979). Heavily silicified rocks containing >0.5 ppm Au are labeled as siliceous Au ores, and <0.5 ppm Au as barren jasperoids. Pyritic samples are defined as having high Fe contents relative to Al, regardless of Au content (Fig. 13D).

Although the presence of dickite-filled fractures in jasperoids demonstrates minor Al mobility in proximal zones, the bulk of Al and probably also Ti has been essentially immobile and is considered to represent the initial clay and detrital components of the host sediments. Both oxidized and unoxidized rocks are plotted in Figure 13A and B because oxidation and leaching by slightly to moderately acid supergene solutions should not modify Al, Ti, or K contents significantly.

The plots show clearly that Ti and K correlate closely with Al. Correlations for 100 samples show correlation coefficients of 0.92 for Ti vs. Al and 0.94 for K vs. Al, and both trends effectively include the origin. Background samples generally have higher K/Al than the well-defined trend for mineralized and altered rocks (Fig. 13B), even though weathering of these surface samples could result in local K depletion. A similar systematic variation in Ti/Al relationships is not apparent (Fig. 13A). The highest Al, Ti, and K contents are restricted to intensely leached rocks which have not been silicified and which have greatly reduced bulk densities. These leached rocks are not necessarily mineralized with Au; however, they usually contain elevated values for As, Tl, Hg, and other trace elements (Table 3). Figure 13A and B emphasize the apparent enrichment problem resulting from progressive carbonate removal during alteration when individual elements are evaluated on a weight percent basis. If Al is assumed to be constant, measured densities demonstrate that the rock has compacted, so that comparisons in mg/cm<sup>3</sup> are also misleading.

Background SiO<sub>2</sub> contents are typically <35 percent; increases occur by both adding SiO<sub>2</sub> and leaching carbonate (Fig. 13C). Background samples and many altered samples have SiO<sub>2</sub>/Al<sub>2</sub>O<sub>3</sub> by weight of about 6, suggesting that the original detrital component averaged this composition. Many leached decalcified samples retain approximately this ratio and have apparently been enriched in Al and SiO<sub>2</sub> by carbonate removal. However, jasperoids, silicified ores, and pyritically altered rocks have all clearly experienced SiO<sub>2</sub> addition through varying degrees of silicification.

Comparison of Figure 13B and C shows that most altered rocks with less than approximately 5 percent Al<sub>2</sub>O<sub>3</sub> are silicified and/or pyritic (note that samples labeled "S," "J," and "P" in Fig. 13C are marked by "o" in lower left portion of Fig. 13B). Relative to the general trend between Fe and Al contents shown in

Figure 13D, samples with elevated Fe contents are pyritic, and samples falling below this trend are restricted to leached proximal samples, in particular, barren footwall.

Two groups of samples showing differing alteration sequences can be distinguished on the basis of  $\text{Al}_2\text{O}_3$  content. In illite-poor carbonate-rich samples with low Al contents, progressive alteration goes from background to pyritic to siliceous. This reflects the tendency for coarser grained, less clay-rich beds such as bioclastic horizons and calcareous siltstones to be selectively pyritized and silicified. In contrast, typical laminated carbonate samples with higher initial clay contents show zones of progressive decalcification and leaching prior to eventual silicification, or in some cases, jasperoid development.

In order to evaluate changes in the quantity of  $\text{SiO}_2$  as quartz, the variable excess  $\text{SiO}_2$  is calculated by deducting  $\text{SiO}_2$  in illite (muscovite) from total  $\text{SiO}_2$ : excess  $\text{SiO}_2$  (wt %) =  $60.08 \times (\text{moles SiO}_2 - 3 \text{ moles K}_2\text{O})$ .

The relationships of carbonate leaching and silicification are illustrated in Figure 14A. Most samples fall

along a trend of decreasing carbonate with increasing quartz, extending from an average background sample (30.8%  $\text{CO}_2$ , 30.0% CaO, 7.3% MgO, 21.2% excess  $\text{SiO}_2$ , and 10.6% other, mostly clay) to a composition with no  $\text{CO}_2$  and 67 percent excess  $\text{SiO}_2$ . This trend is interpreted as being caused by carbonate dissolution. Most jasperoids and silicified ores contain higher values of excess  $\text{SiO}_2$  and <5 percent  $\text{CO}_2$ . The small quantities of  $\text{CO}_2$  in these samples are mainly late-stage calcite. A few silicified samples, mainly reduced ores, have  $\text{SiO}_2$  lower than 67 percent.

The general sequence on this plot from background samples, through decarbonated samples, to silicified samples follows the inferred sequence of progressive alteration. Excess  $\text{SiO}_2$  is therefore a useful variable for examining the changes of other components with progressive alteration.

#### Alteration of Al + K-bearing silicates

The molar ratio  $\text{K}/(\text{K} + \text{Al})$  reflects the stability of the  $\text{Al} \pm \text{K}$ -bearing phases (K feldspar, illite-sericite, dickite-kaolinite) with respect to the hydrothermal

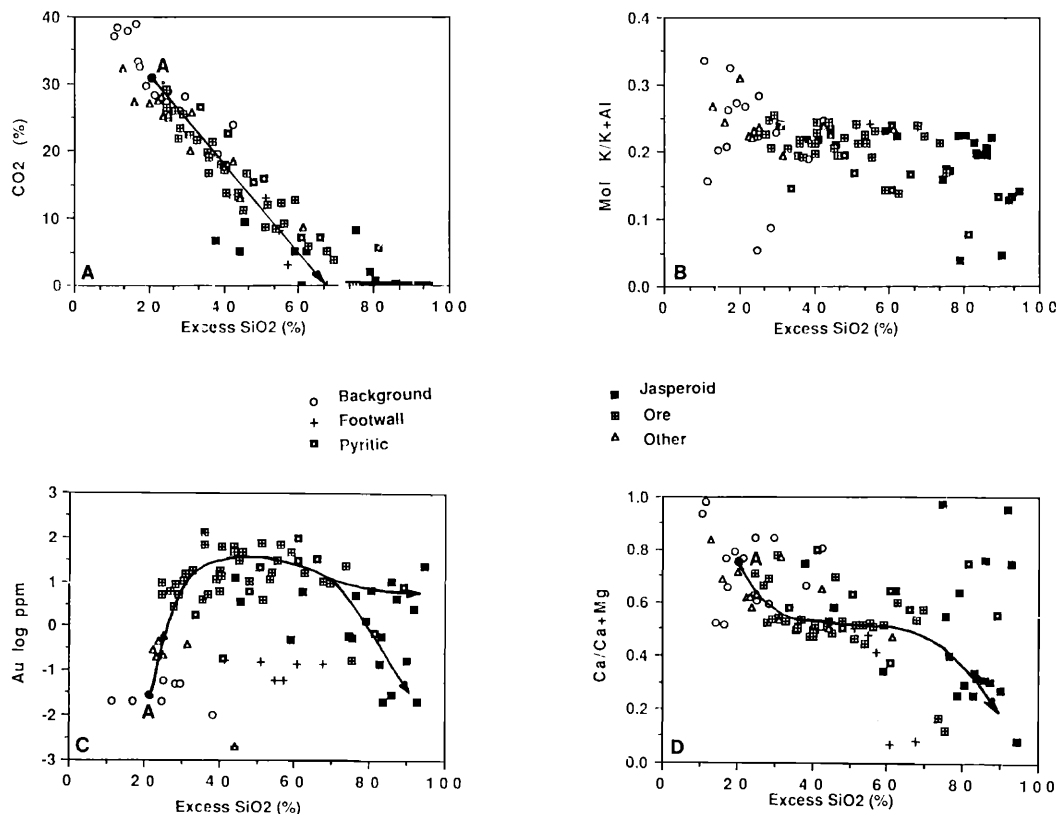


FIG. 14. Relationships of  $\text{CO}_2$ ,  $\text{K}/(\text{K} + \text{Al})$ , log Au (ppm), and  $\text{Ca}/(\text{Ca} + \text{Mg})$  to excess  $\text{SiO}_2$  ("quartz"), for Roberts Mountains Formation of various alteration types. Point "A" is average unaltered Roberts Mountains Formation. Line in A represents calculated effect of carbonate dissolution from unaltered rock. Lines in C and D represent typical paths inferred for progressive alteration as fluid channels are approached.

fluid. Of the common minerals, microcline has a  $K/(K + Al)$  of 0.5, muscovite (illite) of approximately 0.25, and kaolinite of 0.0. Illite can be slightly deficient in K; other feldspars, clays, and aluminosilicates have ratios near 0.0, but, they are scarce at Carlin.

Figure 14B illustrates the variation of  $K/(K + Al)$  plotted against excess  $SiO_2$ . With increasing alteration,  $K/(K + Al)$  decreases from values commonly greater than 0.25 in unaltered rocks, to about 0.25 in the decarbonation zone (assemblages 2 and 3), to 0.22 ( $n = 20$ ) in the siliceous-argillitic zone (assemblage 4) to 0.17 ( $n = 15$ ) in siliceous ores and jasperoids (assemblage 5). This progressive decrease is attributed to illite and K feldspar in unaltered rocks (Mullens, 1979) being converted to illite-sericite in the decarbonation zone, followed by illite-sericite conversion to dickite-kaolinite in the inner zones. Petrographic and SEM-EDS studies of several unoxidized Au ore samples from section 15E show local coarsening of the micas within decalcified rocks containing some dolomite; similar observations were reported by Bakken et al. (1989). Values of  $K/(K + Al)$  are consistent with the dominance of illite-sericite in the partly decarbonated zone and a lack of kaolinite development. The occurrence of nonsilicified, unoxidized rocks having  $K/(K + Al)$  from 0.23 to 0.24 and showing extensive leaching of calcite and dolomite suggests that extensive carbonate removal may occur without appreciable K mica destruction and/or dickite-kaolinite development. Ratios markedly lower than 0.25 in distal rocks are generally restricted to hydrothermally altered coarser siltstone and bioclastic interbeds. This restriction suggests that these more permeable beds are the most intensely altered in a given location.

In the siliceous-argillitic zone, common low  $K/(K + Al)$  values within this zone, combined with the ubiquitous presence of both 0.7 and 1.0 nm XRD peaks, suggest that K mica is being converted to dickite-kaolinite. Silicified ores and jasperoids have  $K/(K + Al)$  ranging from 0.08 to 0.22. Low  $K/(K + Al)$  values correlate with the presence of kaolinite-dickite in most of these samples, which are also relatively low in both K and Al, reflecting their origin as coarser clastic horizons with low amounts of clay, possibly combined with depletion of K and Al.

#### *Pyritization and Fe depletion*

A considerable amount of pyrite at Carlin is diagenetic in origin, as indicated by the ubiquitous presence of pyrite in essentially all specimens of unweathered Roberts Mountains Formation, including unaltered rocks distant from ore (Mullens, 1979). This origin is supported by Figure 13D, showing that in most samples Fe correlates with Al, a clearly sedimentary constituent. The Fe is inferred to have been deposited as Fe-bearing clay and Fe oxide coatings

on clay and to have remained essentially in situ through diagenesis.

Of particular interest in terms of Fe behavior during mineralization are samples falling appreciably off the Fe/Al trend and suggesting hydrothermal addition or depletion of iron. Rocks with elevated Fe/Al are generally siliceous or pyritic ores (as defined by Radtke, 1985), including many bedded jasperoids.

Most pyritic samples are siliceous and enriched in Fe (Fig. 13C); however, they occur across the entire range of carbonate removal. The calcareous siltstones and bioclastic horizons which are pyritized in intermediate to distal zones (Fig. 3) are also the parents for preferentially silicified horizons in more proximal cases (Figs. 9 and 10). This relationship suggests that hydrothermal pyritization is closely related to fluid conduits. Additional evidence for introduction of Fe and S during mineralization is the presence of large amounts of pyrite-marcasite in the deep unoxidized ores of the Lower Post and Betze deposits a few kilometers to the northwest (Bettles, 1989).

Regardless of carbonate content, pyritic samples generally have low  $K/(K + Al)$  values (Table 4), as do most siliceous ores and jasperoids, which suggests that pyritization and silicification may have involved leaching of K in addition to carbonate removal. However, because the relationship of Fe enrichment to carbonate removal and K silicate stabilities is not clear, pyritization defined simply by local addition of Fe and the formation of pyrite does not define a unique spatial alteration zone in Figures 6 and 8.

In contrast to pyritized samples, leached footwall rocks ("L" in Fig. 13D) appear to have lost Fe as well as carbonate. This depletion may be due to minor pyrite dissolution in footwall rocks and Fe redistribution to intermediate zones of alteration (Hausen and Kerr, 1968) as pyrite  $\pm$  marcasite or ferroan rims on dolomite (Armstrong et al., 1987).

#### *Decalcification and silicification alteration*

Interrelationships between  $SiO_2$ , CaO, and MgO are presented in Figure 14D in order to show the chemical effects of both decalcification and silicification. The Y axis  $100(CaO/(CaO + MgO))$  ratio expresses mainly changes in calcite and dolomite content, though minor Mg in clay minerals (chlorite, phengitic sericite, or illite) may be important in carbonate-free samples. Unaltered samples containing calcite plot in the upper left-hand corner of the diagram and those with only dolomite plot near 0.5 on the Y axis.

In general, with increasing intensity of alteration from unaltered to decarbonated to argillized-silicified, samples progress from the upper left to the center of the diagram, and finally to the right edge of Figure 14D. Samples with distal alteration characteristics appear slightly silicified and show slightly lower

TABLE 4. Selected Major Element Data for Pyritized Samples or Samples with Elevated Iron Contents Relative to Al<sub>2</sub>O<sub>3</sub> (according to Fig. 13D)

Sample no.	Au (ppm)	Fe <sub>2</sub> O <sub>3</sub> (wt %)	K/(K + Al) (molar ratio)	Al <sub>2</sub> O <sub>3</sub> (wt %)	K <sub>2</sub> O (wt %)	SiO <sub>2</sub> (wt %)	CaO (wt %)	MgO (wt %)
MUL-6953	NA	2.39	0.204	1.20	0.30	15.3	25.5	16.7
T38-48B	0.19	2.29	0.220	2.07	1.95	43.1	21.2	9.00
CARB-102	0.75	3.56	0.078	0.24	0.02	81.5	5.84	1.42
T38-41B	1.75	2.58	0.148	3.01	0.51	35.7	20.0	10.4
CARB-103	3.26	2.56	0.157	1.82	0.33	73.2	7.87	1.41
RAD-T12-11	6	4.72	0.196	4.20	1.00	51.9	10.3	7.30
RAD-T12-6	8	2.81	0.135	2.50	0.38	90.7	0.26	0.16
T38-59A	21.8	2.07	0.170	2.15	0.43	52.4	13.4	5.70
T38-59B	31	2.07	0.144	2.32	0.38	62.4	6.40	2.54
RAD-T12-12	34	5.06	0.168	4.20	0.83	68.8	6.0	3.20
RAD-T22-8	100	6.81	0.241	10.0	3.10	72.4	1.0	1.20

Samples from this study are all unoxidized bioclastic and/or siltstone interbeds which range from very calcareous (T38-41B, Fig. 3) to intensely silicified (CARB-102); refer to Kuehn (1989) for additional chemical data; NA = not analyzed

Sample description: MUL-6953, oxidized background Roberts Mountains Formation carbonate located 3.2 km southwest of Carlin mine (Mullens, 1979); T38-48B, calcareous bioclastic horizon from unoxidized ore intercept section 15E (Fig. 3, Table 2); CARB-102, carbon-rich bedded jasperoid from unoxidized section described in Figure 9; T38-41B, calcareous siltstone interbed from unoxidized ore intercept section 15E (Fig. 3, Table 2); CARB-103, upper portion of carbon-rich bedded jasperoid shown in Figure 9; RAD-T12-11, sample 11, pyritic ore, from Radtke (1985, p. 50); RAD-T12-6, sample 6, siliceous ore, from Radtke (1985, p. 50); T38-59A, very dark gray to black shale from section 15E (Fig. 11); T38-59B, very dark gray to black shale from section 15E (Fig. 11); RAD-T12-12, sample 12, pyritic ore, from Radtke (1985, p. 50); RAD-T22-8, sample 8, oxidized ore, intensely leached, from Radtke (1985, p. 93)

CaO/(CaO + MgO) values than background samples. Intensely acid-leached rock, or silicified jasperoid devoid of calcite and dolomite and having a little MgO in silicates, plots in the lower right corner. Scatter to the upper right corner arises from late-stage calcite veinlets in heavily silicified rocks such as jasperoids and siliceous ores. Analytical uncertainty also leads to scatter along the Y axis in samples containing very small amounts of CaO and MgO.

#### *Relationship of decalcification and silicification to other alteration features described at Carlin*

**Oxidation:** Major element data for oxidized rocks do not significantly deviate from enrichment or depletion patterns in Figures 13 and 14. Oxidized ores from Radtke (1985, table 22, p. 93) fit nicely into hypogene alteration and mineralization patterns recorded in unoxidized samples.

**Carbon-rich zones:** Organic carbon does not correlate with alteration intensity as measured by the variables of Figures 13 or 14, even when only unoxidized rocks are considered, although many decarbonated samples are somewhat enriched in organic C.

**Late-stage calcite + barite + realgar veins:** Because of the presence of barite in many late-stage calcite and calcite-realgar veins, depletion of samples, with Ba > 1,000 ppm, also removes many of the data points falling in the upper right quarter of Figure 14D.

#### *Relationship of Au, As, and other heavy metals to alteration*

Figure 14C shows the relationship of Au content to excess SiO<sub>2</sub>. The Au concentration increases

abruptly from background levels (1–5 ppb) to over 50,000 ppb in the carbonate depletion zone. Au values higher than several ppm are generally restricted to rocks showing at least slight acid leaching. As seen in Figure 12, coarse-grained bioclastic interbeds generally contain the highest silica and lowest Au values within individual hand samples. This pattern is consistent with the typically low values found in jasperoids and areas of intense silicification (i.e., Bakken and Einaudi, 1986). Massive carbonate beds are typically unmineralized, and moderately to intensely decalcified samples locally have high Au contents; however, intensely leached rocks may contain no Au. In contrast to carbonate-depleted samples in the mineralized zone, footwall carbonate-depleted samples are relatively low in Au (Fig. 14C, Table 3).

The leached footwall rocks contain significant enrichment in trace elements such as As, Hg, Tl, and Sb (Table 3; Kuehn, 1989). This pattern implies either that the process of carbonate dissolution did not cause Au precipitation from the Au-bearing solution or that different fluids were involved in carbonate dissolution and Au deposition.

Two types of evidence show that pyritization is not directly correlated with Au mineralization. Many pyritized argillically altered dikes are not Au bearing. Also, in pyritized sedimentary samples (Table 4), Fe and Au do not correlate closely.

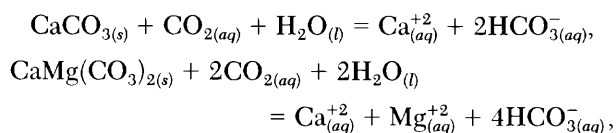
In contradiction to the above, Bakken et al. (1989) clearly documented submicron-sized particles of gold encapsulated within certain types of pyrite in unoxidized high-grade Au ore, refining the relationship between Au and hydrothermal pyrite previously

suggested by Joralemon (1951), Hausen and Kerr (1968), Radtke et al. (1972, 1980), Wells and Mullen (1973), Hausen (1981, 1983, 1985), Radtke (1985), Hausen and Park (1986), Chao et al. (1987), and Hausen et al. (1987).

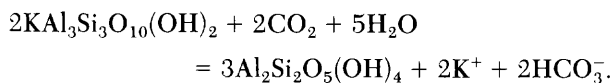
#### *Ore fluid characteristics*

The formation of dickite-kaolinite along hydrothermal conduits and in dikes requires alteration by a fluid with a low K/H and probably a low pH (Rose and Burt, 1979). The marcasite observed in one East pit dike and also reported as a hypogene Fe sulfide at the Deep Post deposit (Bettles, 1989) also indicates a fluid that is acidic and contains appreciable sulfur (Murowchick, 1984; Murowchick and Barnes, 1986). Extensive carbonate removal requires an acidic fluid.

The species responsible for the low pH and extensive carbonate leaching appears to be CO<sub>2</sub>. Kuehn and Rose (1987b) and Kuehn (1989) report fluid inclusions containing about 5 mole percent CO<sub>2</sub> in quartz veins cutting jasperoids and argillically altered dikes in the East pit, at CO<sub>2</sub> pressures of 800 ± 400 bars at temperatures of 215° ± 30°C. This CO<sub>2</sub> amounts to very high concentrations of carbonic acid (H<sub>2</sub>CO<sub>3</sub>) in the fluid, and therefore, a high capacity to leach carbonates and alter silicates by the following types of reactions:



and



Although other workers have postulated shallow boiling of a low-salinity near-neutral solution to form acidic alteration at Carlin (Radtke, 1985; Rye, 1985), the high CO<sub>2</sub> pressures indicated by the fluid inclusions, which require a depth of 4 ± 2 km, and the occurrence of carbonate leaching and dickite formation to depths exceeding 600 m at the Post and Betze deposits are not consistent with shallow boiling. In addition, the deposition of K feldspar in the boiling zone predicted by this model is not observed. The huge amount of acid required to dissolve carbonate is more easily explained by a fluid with 5 mole percent CO<sub>2</sub> (about 3 M) than by any other solute, given that the freezing point of inclusions indicates a dissolved nonvolatile solute content of only about 0.5 M (Kuehn, 1989). Given a typical Na/K ratio of about 10, only about 10<sup>-4.5</sup> M of strong acid could be present in this fluid at the muscovite-kaolinite boundary.

Mobility of K<sup>+</sup> and local K enrichment is poten-

tially reflected by the formation of jarosite in higher levels of the Carlin mine (Hausen, 1967); however, the jarosite could also be supergene. At the Gold Quarry mine, Rota (1987) and Rota and Ekburg (1988) reported zoning from deep mineralized kaolinite (or dickite?) zones upward to a zone containing appreciable alunite and Au, overlain by Au-bearing siliceous ores, but Arehart et al. (1992) show from stable isotopic data and radiometric dating that this alunite is supergene. At the Post deposit, these authors show that alunite and some kaolinite are supergene but that much kaolinite is hypogene. Hydrothermal kaolinite, jarosite, and alunite have also been reported at the Alligator Ridge deposit by Ilchick et al. (1986), but the alunite is supergene according to Arehart et al. (1992).

The carbonate-leached zones are therefore interpreted as alteration envelopes around hydrothermal conduits through which CO<sub>2</sub>-rich solutions traveled. They are not restricted to the upper levels of the Carlin deposit nor are leached rocks necessarily oxidized. As this study shows, distinctly hypogene carbonate leaching and Al ± K silicate alteration must be evaluated separately from any subsequent leaching, kaolinite development, and oxidation due to supergene effects.

Although both the zonation of decalcification and the K ± Al silicate alteration may be caused by hypogene low pH alteration, this interaction does not explain the clear spatial localization of silicification in proximal zones as shown in this study and by Bakken and Einaudi (1986). Because SiO<sub>2</sub> solubility is insensitive to pH over a wide range of pH values, neutralization of an acidic ore fluid due to carbonate dissolution would not lead to deposition of silica (Holland and Malinen, 1979). Although at temperatures less than about 250°C the major control of silica deposition is temperature, the bedding-specific stratiform silicification in footwall rocks is difficult to account for by a simple mine-scale thermal gradient leading to silica deposition, as postulated by Radtke (1985).

The selective replacement along beds of higher permeability suggests that mixing with a second, probably cooler fluid is a more likely cause of silica deposition. Any fluid-fluid interactions are likely to be most intense in zones of greatest permeability. Decompressional CO<sub>2</sub> separation and/or mixing conditions involving different interactions between a hotter, silica- and metal-bearing, CO<sub>2</sub>-rich, low pH fluid and a cooler, volatile-poor, carbonate-stable and perhaps more oxidized fluid, can also explain jasperoid development without complete carbonate removal (i.e., by rapid cooling or quenching). Advanced carbonate leaching without silicification, such as is commonly seen in footwall rocks, would occur in areas where cooling effects due to mixing or decompression are absent.

### Summary and Conclusions

This study shows that hydrothermal flow was controlled by permeable bioclastic horizons in the upper Roberts Mountains Formation, by crosscutting faults, and by rocks fractured as a result of solution collapse. The Au depositional period can be constrained to follow Cretaceous dike emplacement and to predate oxidation of major portions of the deposit. Within the Au depositional stage, early features include jasperoid development and quartz veining in dikes, and these are followed by crosscutting quartz veinlets in jasperoids as well as later barite and calcite veins that in some cases contain As-, Sb-, Hg-, and Tl-bearing phases. Oxidation and bleaching of the rocks are post-ore supergene effects rather than hypogene as indicated by the following evidence: (1) oxidation is limited or blocked by late ore-stage calcite veins, (2) oxidation shows no relation to hypogene alteration and mineralization effects, (3) the major clay mineral formed in unoxidized proximal alteration zones is dickite (a typical hydrothermal clay), (4) oxidation has formed goethitic to amorphous Fe oxide rather than the higher temperature phase, hematite, predicted in hypogene oxidation, (5) oxidation follows permeable structures and beds from the surface, (6) deep ores at Carlin as well as in the Post and Betze deposits of the Goldstrike area lack any oxidation and bleaching, and finally, (7) Bakken et al. (1989) have documented the encapsulation of free gold in pyrite and other sulfides present in unoxidized Au ores from Carlin.

In rocks that contain pyrite and pyrobitumen at Carlin, alteration is zoned around structures and permeable beds in the following generalized sequence: (1) unaltered: quartz + K feldspar + illite + calcite + dolomite, (2) decalcified: quartz + illite + dolomite ± (calcite), (3) decarbonated: quartz + sericite-illite ± (dolomite), (4) siliceous-argillic: quartz + dickite-kaolinite + sericite-illite, and (5) jasperoid: quartz + dickite-kaolinite.

This alteration zoning is controlled by permeability and occurs at a wide range of scales, from tiny fractures through permeable beds to deposit scale. Gold is most commonly enriched in the decalcified and decarbonated zones where calcite and dolomite, respectively, are dissolved, rather than in the more silicified zones, although sporadic high Au contents occur in all zones.

Volume loss due to compaction following the removal of carbonate creates apparent increases in Al, K, Fe, and other elements, but ratios to relatively immobile Al and Ti show little change except for loss of Ca, Mg, CO<sub>2</sub>, and minor K, as well as gain of SiO<sub>2</sub>. Units in the footwall of the ore zone are extensively decarbonated and contain little silicification, pyritization, or Au but high amounts of As, Sb, Hg, and Tl in relation to unaltered rocks.

The presence of dickite along zones of intense alteration and the extensive decarbonation indicate that the ore fluid was distinctly acidic, with an estimated pH of less than 4.5 at 215°C. Fluid inclusions indicate that the acidity of this deep altering fluid was in the form of very high CO<sub>2</sub> contents compared with typical shallow geothermal fluids. Prior suggestions of boiling in an epithermal environment would have increased pH in the lower part of the boiling zone, with resulting tendencies toward conversion of illite-sericite to K feldspar (adularia) rather than to kaolinite-dickite.

Extensive silicification that has a spatial relationship with decarbonation and Au mineralization seems to require decompressional boiling and/or mixing of a cooler water with the hot, CO<sub>2</sub>-rich, Au-bearing fluid from depth in order to cause precipitation. This cooler fluid probably descended along structures as well as the zone of permeable rocks in the upper Roberts Mountains Formation or possibly along the Roberts Mountains thrust fault.

### Acknowledgments

Sincere thanks are extended to the Newmont Gold Company for permission to conduct this research on their property and for considerable assistance while in the field. The list of helpful Newmont personnel is too long to be complete; however, Charles Ekburg, Odin Christensen, and Joe Rota made working at Carlin both possible and enjoyable. Thanks are also given to William C. Bagby and Raul J. Madrid of the U. S. Geological Survey for the open collegial exchange on Carlin-type deposits and the geology of north-central Nevada. Major financial support for this research was provided through National Science Foundation grant EAR-8407743, and field work in 1983 to 1985 was supported in part by the Western Mineral Resources Branch, U. S. Geological Survey.

February 7, 1991; May 27, 1992

### REFERENCES

- Akright, R. L., Radtke, A. S., and Grimes, D. J., 1969, Minor elements as guides to gold in the Roberts Mountains Formation, Carlin gold mine, Eureka County, Nevada: *Colorado School Mines Quart.*, v. 64, p. 49-66.
- Arehart, G. B., Kesler, S. E., Foland, K. A., and Hubacher, F. A., 1989, Alteration zoning and geochronology of the Post micron gold deposit, Nevada [abs.]: *Geol. Soc. America Abstracts with Programs*, v. 21, p. A350.
- Arehart, G. B., O'Neil, J. R., Kesler, S. E., and Foland, K. A., 1991, Supergene alunite from sediment-hosted micron gold deposits, western U.S.A. [abs.]: *Geol. Assoc. Canada Program with Abstracts*, v. 16, p. A4.
- Arehart, G. B., Kesler, S. E., O'Neil, J. R., and Foland, K. A., 1992, Evidence for the supergene origin of alunite in sediment-hosted micron gold deposits, Nevada: *ECON. GEOL.*, v. 87, p. 263-270.
- Armstrong, A. K., Bagby, W. C., Ekburg, C., and Repetski, J., 1987, Petrographic and scanning electron microscope studies of samples from the Roberts Mountains and Popovich Formations,

- Carlin mine area, Eureka Co., NV: U. S. Geol. Survey Bull. 1684, 23 p.
- Bakken, B. M., 1990, Gold mineralization, wallrock alteration and the geochemical evolution of the hydrothermal system in the Main ore body, Carlin mine, Nevada: Unpub. Ph.D. thesis, Stanford Univ., 200 p.
- Bakken, B. M., and M. T. Einaudi, 1986, Spatial and temporal relations between wall-rock alteration and gold mineralization, main pit, Carlin gold mine, Nevada, in Macdonald, A. J., ed., *Gold '86: Willowdale, Ontario*, Konsult Internat., p. 388-403.
- Bakken, B. M., Hochella, M. F., Jr., Marshall, A. F., and Turner, A. M., 1989, High-resolution microscopy of gold in unoxidized ore from the Carlin mine, Nevada: *ECON. GEOL.*, v. 84, p. 171-180.
- Bettles, K. H., 1989, Gold deposits of the Goldstrike mine, Carlin Trend, Nevada: *Am. Inst. Mining Engineers-Soc. Mining Engineers Ann. Mtg.*, Las Vegas, NV, Feb. 27-March 2, 1989, preprint 89-158, 14 p.
- Chao, E. T. C., Chen, J. R., Minkin, J. A., and Back, J. M., 1987, Synchrotron and micro-optical studies of the occurrence of gold in Carlin-type ore samples: Implications for processing and recovery, in Vassililou, A. H., Hausen, D. M., and Carson, D. J. T., eds., *Process mineralogy VII: Warrendale, Pennsylvania*, Metall. Soc., Am. Inst. Mining Engineers Press, p. 143-152.
- Christensen, O. D., Knutsen, G. C., and Ekburg, C. E., 1987, Disseminated gold deposits of the Carlin trend, Eureka and Elko Counties, Nevada: *Am. Inst. Mining Engineers-Soc. Mining Engineers Ann. Mtg.*, Denver, CO, Feb. 24-27, 1987, preprint 87-84, 7 p.
- Dhooge, P. M., and Park, S. M., 1983, Electrochemistry of coal slurries II. Studies on various parameters affecting oxidation of coal slurries: *Electrochem. Sci. Technology*, v. 130, p. 1029-1036.
- Dhooge, P. M., Stilwell, D. E., and Park, S. M., 1982, Electrochemistry studies of coal slurry oxidation mechanisms: *Electrochem. Sci. Technology*, v. 129, p. 1719-1724.
- Evans, J. G., 1974a, Geologic map of the Rodeo Creek NE quadrangle, Eureka County, Nevada: U. S. Geol. Survey Geol. Quad. Map GQ-1116, scale 1:24,000.
- 1974b, Geologic map of the Welches Canyon quadrangle, Eureka County, Nevada: U. S. Geol. Survey Geol. Quad. Map GQ-1117, scale 1:24,000.
- 1980, Geology of the Rodeo Creek NE and Welches Canyon quadrangles, Eureka County, Nevada: U. S. Geol. Survey Bull. 1473, 81 p.
- Evans, J. G., and Peterson, J. A., 1986, Distribution of minor elements in the Rodeo Creek NE and Welches Canyon quadrangles, Eureka County, Nevada: U. S. Geol. Survey Bull. 1657, 65 p.
- Hausen, D. M., 1967, Fine gold occurrence at Carlin, Nevada: Unpub. Ph.D. thesis, Columbia Univ., 166 p.
- 1981, Process mineralogy of auriferous pyritic ores at Carlin, Nevada, in Hausen, D. M., and Park, W. C., eds., *Process mineralogy, extractive metallurgy, mineral exploration, energy resources: Warrendale, Pennsylvania*, Metall. Soc., Am. Inst. Mining Engineers Press, p. 279-289.
- 1983, Process mineralogy of auriferous pyrite: *Geol. Soc. South Africa Spec. Pub.* 7, p. 261-269.
- 1985, Process mineralogy of select refractory Carlin-type ores: *Canadian Mining Metall. Bull.*, v. 78, no. 881, p. 83-94.
- Hausen, D. M., and Kerr, P. F., 1968, Fine gold occurrence at Carlin, Nevada, in Ridge, J. D., ed., *Ore deposits of the United States 1933-1967 (Graton-Sales vol.)*: New York, Am. Inst. Mining Metall. Petroleum Engineers, p. 908-940.
- Hausen, D. M., and Park, W. C., 1986, Observations on the association of gold mineralization with organic matter in Carlin-type ores: *Soc. Denver Region Explor. Geologists Proc.*, v. 2, p. 119-136.
- Hausen, D. M., Ekburg, C., and Kula, F., 1983, Geochemical and XRD-logging method for lithologic ore type classification of Carlin-type gold ores, in Hagni, R. D., ed., *Process mineralogy II: Warrendale, Pennsylvania*, Metall. Soc., Am. Inst. Mining Engineers Press, p. 421-450.
- Hausen, D. M., Ahlrichs, J. W., Mueller, W., and Park, W. C., 1987, Particulate gold occurrences in three Carlin carbonaceous ore types, in Hagni, R. D., ed., *Process mineralogy VI: Warrendale, Pennsylvania*, Metall. Soc., Am. Inst. Mining Engineers Press, p. 193-214.
- Holland, H. D., and Malinin, S. D., 1979, The solubility and occurrence of non-ore minerals, in Barnes, H. L., ed., *Geochemistry of hydrothermal ore deposits: New York, Wiley Intersci.*, p. 461-508.
- Ilchick, R. P., Brimhall, G. H., and Schull, H. W., 1986, Hydrothermal maturation of indigenous organic matter at the Alligator Ridge gold deposits, Nevada: *ECON. GEOL.*, v. 81, p. 113-130.
- Joralemon, P., 1951, The occurrence of gold at the Getchell mine, Nevada: *ECON. GEOL.*, v. 46, p. 267-310.
- Knutsen, G. C., Zimmerman, C. J., and Christensen, O. D., 1991, Current geologic research and deep deposits of the Carlin trend, northeast Nevada: *The Gangue (Geol. Assoc. Canada, Mineral Deposits Branch)*, no. 34, p. 3-5.
- Kuehn, C. A., 1989, Studies of disseminated gold deposits near Carlin, Nevada: Evidence for a deep geologic setting of ore formation: Unpub. Ph.D. thesis, Pennsylvania State Univ., 395 p.
- Kuehn, C. A., and Rose, A. W., 1986, Temporal framework for the development of fluids at the Carlin gold mine, Eureka County, Nevada [abs.]: *Geol. Soc. America Abstracts with Programs*, v. 18, p. 663.
- 1987a, Temporal relationships between hydrocarbon introduction and maturation and gold mineralization/alteration at Carlin, Nevada: A tale of two fluids [abs.], in Vassililou, A. H., Hausen, D. M., and Carson, D. J. T., eds., *Process mineralogy VII: Warrendale, Pennsylvania*, Metall. Soc., Am. Inst. Mining Engineers Press, p. 161.
- 1987b, Chemical and mineralogical zonation associated with low pH hydrothermal alteration at the Carlin Gold deposit, NV [abs.]: *Geol. Soc. America Abstracts with Programs*, v. 19, p. 734.
- Langmuir, D., 1971, Particle size effect on the reaction goethite = hematite + water: *Am. Jour. Sci.*, v. 271, p. 147-156.
- Loving, T. S., 1949, Rock alteration as a guide to ore: *ECON. GEOL. MON.* 1, 63 p.
- Madrid, R. J., 1987, Stratigraphy of the Roberts Mountains allochthon in north-central Nevada: Unpub. Ph.D. thesis, Stanford, California, Stanford Univ., 332 p.
- Madrid, R. J., and Bagby, W. C., 1986, Structural alignment of sediment-hosted gold deposits in north-central Nevada: An example of inherited fabrics [abs.]: *Geol. Soc. America Abstracts with Programs*, v. 18, p. 392.
- Matti, J. C., and McKee, E. H., 1977, Silurian and Lower Devonian paleogeography of the outer continental shelf of the Cordilleran miogeosyncline, central Nevada, in Stewart, J. H., Stevens, C. H., and Fritsche, A. E., eds., *Paleozoic paleogeography of the western United States: Soc. Econ. Paleontologists Mineralogists, Pacific Sec., Pacific Coast Paleogeography Symposium*, Bakersfield, California, April 22, 1977, v. 1, p. 181-215.
- McKee, E. H., Silberman, M. L., Marvin, R. E., and Obradovich, J. D., 1971, A summary of radiometric ages of Tertiary volcanic rocks in Nevada and eastern California. Part 1—central Nevada: *Isochron/West*, no. 2, p. 21-42.
- Medlin, J. H., Suhr, N. H., and Bodkin, J. B., 1969, Atomic absorption analysis of silicates employing LiBO<sub>2</sub> fusion: *Atomic Absorption Newsletter*, v. 8, no. 2, p. 25-29.
- Morrow, A. B., and Bettles, K., 1982, Geology of the Goldstrike mine, Elko County, Nevada: Northwest Mining Convention Ann. Mtg., Spokane, Washington, Dec. 10, 1982, preprint, 4 p.
- Mullens, T. E., 1979, Mineralogic and chemical composition of

- 246 samples of the laminated limestone unit of the Roberts Mountains Formation and related formations, north-central Nevada: U. S. Geol. Survey Open-File Rept. 79-753, 4 sheets.
- 1980, Stratigraphy, petrology, and some fossil data of the Roberts Mountains Formation, north-central Nevada: U. S. Geol. Prof. Paper 1063, 67 p.
- Murowchick, J. B., 1984, The formation and growth of pyrite, marcasite, and cubic FeS: Unpub. Ph.D. thesis, Pennsylvania State Univ., 168 p.
- Murowchick, J. B., and Barnes, H. L., 1986, Marcasite precipitation from hydrothermal solutions: *Geochim. et Cosmochim. Acta*, v. 50, p. 2615-2629.
- Radtke, A. S., 1985, Geology of the Carlin gold deposit, Nevada: U. S. Geol. Survey Prof. Paper 1267, 124 p.
- Radtke, A. S., Heropoulos, C., Fabbi, B. P., Scheiner, B. J., and Essington, M., 1972, Data on major and minor elements in host rocks and ores, Carlin gold deposit, Nevada: *ECON. GEOL.*, v. 67, p. 975-978.
- Radtke, A. S., Rye, R. O., and Dickson, F. W., 1980, Geology and stable isotope studies of the Carlin gold deposit, Nevada: *ECON. GEOL.*, v. 75, p. 641-672.
- Regnier, J., 1960, Cenozoic geology in the vicinity of Carlin, Nevada: *Geol. Soc. America Bull.*, v. 71, p. 1189-1210.
- Roberts, R. J., 1960, Alinement of mining districts in north-central Nevada: U. S. Geol. Survey Prof. Paper 400-B, p. B17-B19.
- Rose, A. W., and Burt, D. M., 1979, Hydrothermal alteration, in Barnes, H. L., ed., *Geochemistry of hydrothermal ore deposits*: New York, Wiley Intersci., p. 173-227.
- Rose, A. W., and Kuehn, C. A., 1987, Ore deposition from acidic CO<sub>2</sub>-rich solutions at the Carlin gold deposit, Eureka County, Nevada [abs.]: *Geol. Soc. America Abstracts with Programs*, v. 19, p. 824.
- Rota, J. C., 1987, Geology of Newmont Gold Company's Gold Quarry deposit, Eureka County, Nevada, in Elliott, I. L., and Smee, B. W., eds., *GeoExpo '86, Exploration in the North American Cordillera*: Rexdale, Canada, Assoc. Exploration Geochemists, p. 42-50.
- Rota, J. C., and Ekburg, C. E., 1988, History and geology outlined for Newmont's Gold Quarry deposit in Nevada: *Mining Eng.*, v. 40, p. 239-245.
- Rye, R. O., 1985, A model for the formation of carbonate-hosted disseminated gold deposits based on geologic, fluid-inclusion, geochemical, and stable-isotope studies of the Carlin and Cortez deposits, Nevada: U. S. Geol. Survey Bull. 1646, p. 95-105.
- Sato, M., and Mooney, H. M., 1960, The electrochemical mechanism of sulfide self-potentials: *Geophysics*, v. 25, p. 226-245.
- Sheppard, T. L., and Zimmerman, C. J., 1988, The geology and mineralogy of the Genesis gold deposit [abs.]: *Am. Inst. Mining Engineers Ann. Mtg.*, Phoenix, Arizona, Jan. 25-28, 1988, Abstracts with Program, p. 130.
- Silberman, M. L., and McKee, E. H., 1971, K-Ar ages of granitic plutons in north-central Nevada: *Isochron/West*, no. 71-1, p. 15-32.
- Wells, J. D., and Mullens, T. E., 1973, Gold-bearing arsenian-pyrite determined by microprobe analysis, Cortez and Carlin gold mines, Nevada: *ECON. GEOL.*, v. 68, p. 187-201.
- Zoback, M. L., Anderson, R. E., and Thompson, G. A. 1981, Cainozoic evolution of the state of stress and style of tectonism of the Basin and Range province of the western United States: *Royal Soc. [London] Philos. Trans.*, v. 300, no. 1454, p. 407-434.